



Reductive Photocatalysis and Smart Inks

Journal:	<i>Chemical Society Reviews</i>
Manuscript ID:	CS-TRV-08-2014-000279.R1
Article Type:	Tutorial Review
Date Submitted by the Author:	20-Aug-2014
Complete List of Authors:	Mills, Andrew; Queen's University, Wells, Nathan; Queens University Belfast, Chemistry and Chemical Engineering

Reductive Photocatalysis and Smart Inks

Andrew Mills* and Nathan Wells

School of Chemistry and Chemical Engineering, David Keir Building, Stranmillis Road, Belfast, BT18 9ET

andrew.mills@qub.ac.uk

Abstract

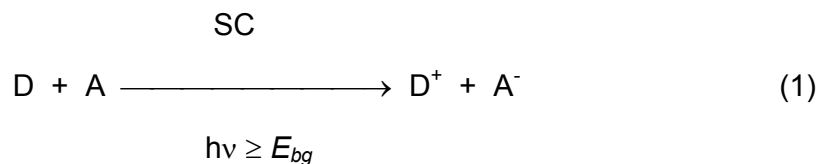
Semiconductor-sensitised photocatalysis is a well-established and growing area of research, innovation and commercialisation; the latter being mostly limited to the use of TiO_2 as the semiconductor.¹⁻⁴ Most of the work on semiconductor photocatalytic systems uses oxygen as the electron acceptor and explores a wide range of electron donors; such systems can be considered to be examples of *oxidative* photocatalysis, *OP*.⁵ *OP* underpins most current examples of commercial self-cleaning materials, such as: glass, tiles, concrete, paint and fabrics. *OP*, and its myriad of applications, have been reviewed extensively over the years both in this journal² and elsewhere^{1,4}. However, the ability of TiO_2 , and other semiconductor sensitiser, to promote *reductive* photocatalysis, *RP*, especially of dyes, is significant and, although less well-known, is of growing importance. In such systems, the source of the electrons is some easily oxidised species, such as glycerol. One recent, significant example of a *RP* process is with respect to photocatalyst activity indicator inks. *paais*, which provide a measure of the activity of a photocatalytic film under test *via* the rate of change of colour of the dye in the ink coating due to irreversible *RP*.^{6,7} In contrast, by incorporating the semiconductor sensitiser *in* the ink, rather than *outside* it, it is possible to create an effective UV dosimeter, based on *RP*, which can be used as a sun-burn warning indicator.⁷ In the above examples the dye is reduced *irreversibly*, but when the photocatalyst *in* an ink is used to *reversibly* photoreduce a dye, a novel, colourimetric oxygen-sensitive indicator ink can be created, which has commercial potential in the food packaging industry.⁸ Finally, if no dye is present in the ink, and the semiconductor photocatalyst-loaded ink film coats an easily reduced substrate, such as a metal oxide film, then it can be used to reduce the latter and so, for example, clean up tarnished steel.⁹ The above are examples of smart inks, i.e. inks that are active and provide either dynamic information (such as UV dose or O_2 level) or a useful function (such as tarnish removal), and all work via a *RP* process and are reviewed here.

1. Introduction

Semiconductor sensitised photocatalysis, or *heterogeneous photocatalysis*, is usually more simply referred^{10,11} to as '*photocatalysis*' and is the acceleration of a redox reaction by a photoexcited semiconductor. Most reports on photocatalytic systems focus on either the oxidation step (as in *oxidative photocatalysis*, *OP*) or, much less often, the reduction step (*reductive photocatalysis*, *RP*), although both are just one part of an overall two-part photocatalysed redox reaction. The basic principles of photocatalysis and the reasons behind the above categorisation of photocatalytic reactions, are outlined in the next section.

2. Oxidative and reductive semiconductor photocatalysis

The basic principles of semiconductor photocatalysis, as summarised by the schematic in figure 1, have been reported by many^{1-6, 10} and so will only be discussed briefly here. Thus, in semiconductor photocatalysis: radiation of energy greater or equal to the band gap, E_{bg} , of the semiconductor, SC, is adsorbed, thereby generating an electron-hole pair (process I in figure 1). The usual fate of the latter is recombination with the concomitant generation of heat and/or light; although with anatase TiO₂ it is usually just heat that is generated (process III). In order for a photocatalytic reaction to occur, some of the photogenerated electrons and holes must reach the surface of the semiconductor and react with an adsorbed electron acceptor, A, (process II_a) and an electron donor, D, (process II_b), respectively. Under such circumstances, the semiconductor particles are said to have photocatalysed the following general redox reaction:

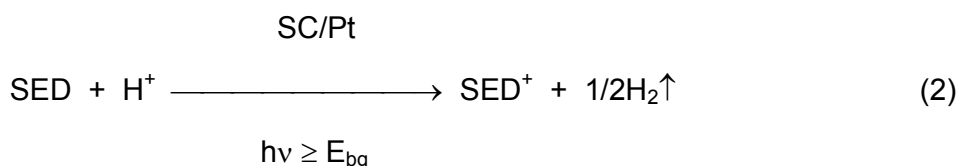


In most cases of photocatalysis, the SC is anatase TiO₂, which has a bandgap of 3.2 eV ($\equiv 388 \text{ nm}$)¹ and the electron acceptor is oxygen, often provided by ambient air. In such systems, invariably the focus is on the oxidation of the electron donor, as it is usually assumed the oxygen is present in such an excess and so easily reduced, that it doesn't play a part in the rate determining step. As a consequence, these systems are sometimes referred⁵ to as examples of *oxidative* photocatalysis, *OP*. Interestingly, as an aside, in such *OP* systems the reduction of oxygen can often prove to be the rate determining step, either due to the slow kinetics of its reduction or its slow diffusion to the surface of the semiconductor, exacerbated, of course, in aqueous solution studies at least, by its low solubility and low diffusion coefficient in water¹.

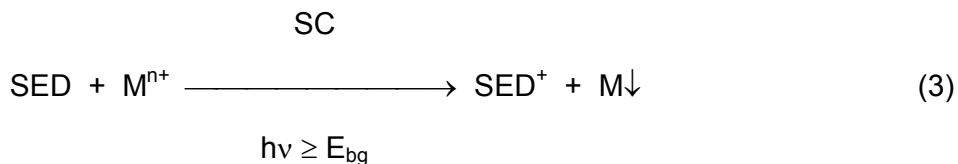
The number of commercial products based on *OP*, with oxygen as the electron acceptor, is extensive and fall under one or more of the following different

categories:¹¹ (1) self-cleaning, architectural materials, such as paint, coated glass, coated tiles, coated or embedded concrete and coated or embedded fabrics (usually awnings), (2) antimicrobial coatings (usually paints and sprays), (3) air purification materials (such as: coated and embedded concrete, coated tiles, air-purifiers), (4) antifogging glass (usually coated mirrors) and (5) water purification systems.

The converse of *OP*, i.e. *reductive* photocatalysis, *RP*, is much less well studied, except for two particular reactions, namely: the photoreduction of water¹², i.e.



and, the photocatalytic reduction of metal ions, usually resulting in the deposition of metals onto the surface of the semiconductor photocatalyst¹³, i.e.



where, SED is a sacrificial electron donor and SED⁺ is its oxidised form that irreversibly decomposes, or is very unreactive, so as to prevent/minimise the back reaction; the SED is usually an alcohol, EDTA or cysteine. Note that for most of the reported systems for the photocatalysed reduction of water, a catalyst, such as Pt, is deposited onto the surface of semiconductor photocatalyst to facilitate the hydrogen evolution reaction, since the overpotential for this reaction on the SC alone is usually so large that reaction (2) would not proceed otherwise.¹⁴ Although most work on reactions (2) and (3) has been conducted using TiO₂, other SCs used for this purpose include: SrTiO₃ and CdS.¹⁵ The photocatalysed reduction of transition metals ions, usually in aqueous solution, i.e. reaction (3), has been very well studied and many metals such as: gold, mercury, silver, platinum, copper and nickel, have been deposited onto the surface of a SC photocatalyst in this way.¹³ It has even been proposed as a method of separation and recovery of precious metals, such as found in jewellers waste.¹⁶ Examples of these reactions and some of the other, albeit very limited, well-established *RP* reactions that have been reported to date are listed in Table 1.¹⁷⁻²²

More recently, using glycerol as the SED, a number of smart inks have been developed based on *RP*. Smart inks are inks that provide useful analytical information or serve a useful active function. The most significant of these *RP*-based smart inks, are photocatalyst activity inks, *paiis*, which provide a measure of the activity of a photocatalytic film under test *via* the rate of change of colour of the dye in the ink coating.⁶ Indeed, *paiis* are now commercially available and also form the basis of a CEN standard under current development^{6,23}. In contrast, by actually

incorporating the semiconductor photocatalyst as particles *in* the ink, not outside it, it is possible to create an effective UV dosimeter, based on *RP*, which can be used as a sun-burn warning indicator.⁷ In the above examples, the dye under observation is reduced *irreversibly*. However, when a dye is used, such as methylene blue (MB), that can be reduced *reversibly* by *RP*, and then be reoxidised by ambient oxygen in the dark, a novel, colourimetric, UV-activated, oxygen-sensitive indicator ink can be created, which has commercial potential in the food packaging industry.⁸ Finally, if no dye is present in the ink, and the semiconductor photocatalyst-loaded ink film coats an easily reduced substrate, such as a metal oxide film, then, upon irradiation, the ink film can reduce the latter and so be used to clean up the tarnished metal.⁹ The following sections provide further details of these examples of smart inks based on *RP*, which is the subject of this review.

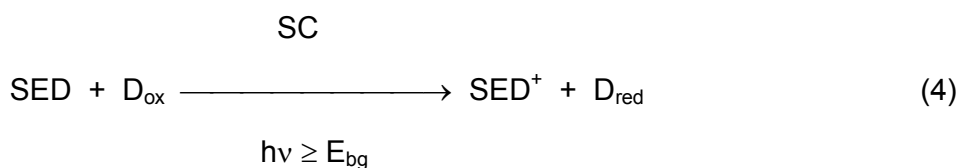
3. Photocatalyst activity indicator inks (*Paiis*)

As noted in section 2, there are now many different commercial photocatalytic products on the market, most, if not all, of which operate via *OP*.^{11-16, 24} The problem with many of these products, such as self-cleaning glass and tiles, is that they are not particularly active, for a variety of reasons including production demands which result in non-ideal values (for maximum photocatalytic activity) in key parameters, such as: film thickness, morphology, crystalline phase and particle size. For example, the low activity of most commercial self-cleaning photocatalytic materials is largely because the TiO₂ photocatalytic coatings have to be tough and hard wearing and as a result are produced in the form of smooth and non-porous coatings, with a resulting low effective reaction surface area on which the photocatalytic process can occur. In addition, quite often the coatings on glass have to be very thin, so as not to alter the optical properties, like reflectivity, of the underling plain glass supporting material. Thus, self-cleaning glass uses as its photocatalytic active layer, usually only a *ca.* 15-20 nm, non-porous coating of 30 nm diameter TiO₂ particles, usually generated by CVD or reactive sputtering.²⁵ As a consequence, the amount of UV absorbed by such a layer is low, e.g. for self-cleaning glass it can be calculated that the fraction of UV light absorbed even at 320 nm is only *ca.* 5% for 20 nm film, assuming the absorption coefficient of titania at this wavelength is *ca.* $2.6 \times 10^4 \text{ cm}^{-1}$.²⁶ Although commercial self-cleaning tiles usually employ a thicker titania layer (*ca.* 100-200 nm), the higher annealing temperature (600-800°C) employed to create the required robust coating causes significant particle sintering, so that the particles are typically of the same size as the film thickness, and such particles are much more light scattering, with a much lower specific surface area.²⁴ As a consequence of the low activities exhibited by many commercial photocatalytic products, it is difficult to demonstrate and/or test the efficacy of such materials in a simple, striking and rapid (typically < 10 min) way.

The problem of finding an effective, rapid method of demonstrating and/or testing photocatalytic activity of such materials is further exacerbated by the fact that many of the organic pollutants, like fats and oils that deposit on glass and tiles, are not

easily destroyed and involve the transfer of many electrons. For example, the photocatalysed complete oxidative mineralisation of stearic acid, a fatty acid found in fingerprints amongst many other things, involves the transfer of 104 electrons from the stearic acid to oxygen. In contrast, the photocatalysed oxidation of most SEDs involves the transfer of far fewer electrons and the generation of fewer intermediates with the result that the process is much more facile. For example, the oxidation of glycerol to glyceraldehyde is a two electron transfer process and transient absorption studies suggest its ability to trap photogenerated holes on TiO₂ occurs on the ns timescale.²⁷

Interestingly, the *reduction* of many dyes to a stable, differently coloured (usually colourless) product is often a two electron step and the coupling of a facile oxidation process, such as that of an SED like glycerol, with a facile reduction process, such as that of a dye, so as to produce a striking colour change, upon ultra-bandgap irradiation of the photocatalyst, is well-established in the solution phase, see table 1.²² Photocatalyst activity indicator inks, *paiis*, work on the same basis as the latter reaction,²⁸⁻³¹ but with the SED and redox indicator dye contained inside the ink coating the SC photocatalyst film under test. Figure 2 illustrates the basic electron transfer reactions that operate in a *paii*, coating a semiconductor photocatalyst film, where SC is usually TiO₂. The redox indicator dye, D_{ox}, is chosen so that it is easily and *irreversibly* reduced to D_{red}, by the photogenerated conduction band electrons ($E^{\circ} = -0.2 \text{ V vs SHE for anatase TiO}_2$)³² on the underlying SC film under test. Whilst the photogenerated holes react irreversibly with the SED in the ink, usually present in vast excess, compared with the dyes. As a result, upon UV irradiation of a *paii*-coated SC, photocatalytically active film, a rapid, striking colour change usually ensues, since one of the essential features of a redox indicator dye is that D_{ox} and D_{red} are very differently coloured. The overall photocatalysed reaction for a *paii* can be summarised as follows:



Reaction (4) is an example of *RP*, because the focus of the overall photocatalytic process is on the reduction of the redox dye and the SED is present in vast excess and so its oxidation is likely to be non-rate-determining.

The components that make up a *paii* must satisfy a number of stringent requirements. For example, the redox dye in its original oxidised and final photoreduced forms should be: (i) as noted above, very readily and irreversibly reduced by the photogenerated electrons (ii) photostable, (iii) not strongly absorbing in the UVA region – which is the usual radiation used to test for photocatalytic activity, (iv) not quenched electronically by the SED or encapsulating polymer and (v) very effective in competing with dissolved oxygen in the ink film for reaction with the

photogenerated conductance band electrons. The latter feature is important, as the ink needs to be able to operate under ambient conditions, i.e. in air and, fortunately, this is not so difficult to achieve since: (i) the dye concentration (typically 0.05 M) is usually much greater than that of oxygen, which is sparingly soluble in the ink, (ii) the dye is usually more strongly adsorbed on the surface of the semiconductor than the oxygen, and (iii) the dye is selected on the basis that, amongst other things, its reduction is a facile process, whereas the reduction of oxygen is slow, although both are irreversible. Other requirements include: the SED must react rapidly and irreversibly with the photogenerated valence band holes ($E^{\circ} = 3.0$ V vs SHE for anatase TiO_2), not absorb significantly in the UVA or visible regions of the solar spectrum, and not quench the electronically excited state of the dye, in either its reduced or oxidised forms. Finally, the encapsulating polymer should be chemically inert, but able to retain water, which usually plays an important part as a proton source in the overall photocatalysed redox reaction.

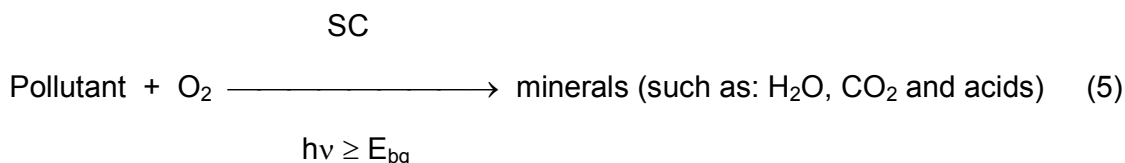
3.1 The resazurin (Rz) *paii*

In 2005, the Mills group published²⁸ the first example of a *paii*, based on the dye resazurin (Rz), which is an oxazone dye, blue/purple in colour (above pH 6.5), and known for its ready and *irreversible* reduction to resorufin (Rf), $E^{\circ}(\text{Rz}/\text{Rf}) = -0.02$ V which is pink in colour. The structure of Rz and some of its spectral details are given in table 2. A typical Rz *paii* comprises: 3 g of a 1.5 wt% aqueous solution of hydroxyl ethyl cellulose (HEC), 0.3 g of glycerol (the SED) and 3 mg of Rz. In an initial study, this ink was applied to both a piece of self-cleaning glass (Pilkington Glass Activ™) and plain glass using a rubber stamp with a flower motif and then irradiated with a UVA lamp (12.4 mW cm^{-2}). The subsequent changes in the colour of the ink were recorded using digital photography and the results of this work are illustrated in figure 3, which show that, under these conditions, the Rz ink rapidly, within 3 min, changes from blue to pink (due to the formation of Rf) when it is in contact with a photocatalyst film, but not on plain glass. The underlying processes that are responsible for this colour change are summarised by the schematic illustration in figure 2 and, more succinctly, by reaction (4). Prolonged irradiation leads to the eventual bleaching of the pink Rf, as it is further, but more slowly, photo-reduced to dihydro-resorufin and other reduced forms.

The data illustrated in figure 3 was obtained under otherwise ambient conditions, i.e. in air, which is a necessary practical requirement of all *paiis*, and indicates that dissolved oxygen does not compete effectively with Rz for reaction with the photogenerated conductance band electrons on the TiO_2 . The Rz/glycerol/HEC *paii* works^{6, 28, 29} rapidly for photocatalyst films of *moderate* photocatalytic activity, such as that exhibited by most examples of commercial self-cleaning glass, like Activ™, see figure 3. It follows that the Rz *paii* can be used as a marketing or quality control tool, or counterfeit detector, for such materials. This qualitative analysis capability is useful, but much more desirable is the ability to provide a measure of the

photocatalytic activity of the material under test, i.e. a quantitative activity analysis capability.

As noted earlier, the photocatalytic mineralisation of pollutants, usually organics, is an *OP* process that underpins **all** current commercial photocatalytic products, such as self-cleaning glass, paint, tiles and concrete, i.e.



It follows that the main concern with using a *paii*, to assess the photocatalytic activity of a new SC material is that, as it works, instead, *via* a *RP* process, although both *OP* and *RP* are both examples of overall photocatalysed redox processes. Thus, it might be argued, any assessment of activity of a photocatalyt's activity made using a *paii* may not necessarily be related simply and directly to the ability of the same material to perform its advertised photocatalytic function, namely the photocatalytic *oxidation* of pollutants via reaction (5). However, as both reactions (4) and (5) are just two examples of the same process, namely: photocatalysis, i.e. 'the acceleration of a redox reaction by a photoexcited semiconductor', it would seem reasonable to assume a high degree of correlation between the two. It follows that, ideally, when using a *paii* to assess the activity of a photocatalytic material, it is better if it has been established previously that this activity measurement correlates with that for an *OP* process which the material has been designed to address, such as, say, the photocatalytic oxidation of: stearic acid (for self-cleaning materials), NO_x (air purification) or MB in solution (water purification).

For example, in the case of the Rz ink and self-cleaning glass, its usefulness to the industry was significantly enhanced once it was established that the measured initial rate of dye reduction, R_{ink} , where R_{ink} = the initial rate of change of absorbance due to the Rz ink at 610 nm, correlates directly with the initial rate of removal a typical organic pollutant used in the assessment of activity of self-cleaning glass, such as stearic acid, as illustrated by the results in figure 4.²⁸ In this work the necessary series of CVD coated samples of anatase titania film on glass samples, with different photocatalyst activities, were prepared by varying the deposition conditions. Note also that the R_{ink} data were obtained in a few minutes, whereas the R_{SA} data required hours under the same illumination conditions.

3.2 The Rz ink: digital photography and K-bar coating

The use of an Rz ink for qualitative analysis, e.g. identifying if an active photocatalyst layer is present, is simple in that detection can be carried out by eye. In contrast, the use of an Rz ink to provide an assessment of the activity of a photocatalytic film requires usually UV/Vis spectrophotometry in order to monitor the photocatalysed colour change of the ink. The latter technique is not inexpensive and requires the

sample to be optically transparent. For opaque samples, such as photocatalytic tiles and paint, diffuse reflectance UV/Visible spectrophotometry can be used instead, but is also not inexpensive in terms of initial outlay for the necessary piece of analytical instrumentation.³⁰

The above spectroscopic requirements appear to present a barrier to the ready adoption of *paiis* for the *quantitative* assessment of the activity of photocatalytic materials, in the lab and, especially, *in situ*. However, recent work^{29, 31} has shown that it is possible to use the much less expensive, more available and easy to use technique of digital colour photography instead to monitor the colour change and produce the necessary high quality analytical data. In digital photography, the image is made up of red (R), green (G) and blue (B) components, i.e. RGB, and usually, for any one *paii*, at least one of these components varies significantly during the colour-changing process so that it can be used to monitor the progress of the photocatalysed colour reaction involving the *paii*. Although a stand-alone digital camera, or even a mobile phone, can be used to generate the necessary digital images, most current work on *paiis* uses a hand-held scanner, although a desk-top scanner is also very effective.

Another potential barrier to the ready application of the *paii* technology for the quantitative assessment of the activities of photocatalytic films is the need for the reproducible production of ink films of the same thickness, since the measured rate of dye bleaching is inversely dependent upon this parameter. In the early work²⁹ on *paiis*, in order to ensure a constant ink film thickness, the ink films were coated onto the photocatalyst films under test using a spin-coating technique. However, spin coaters are not inexpensive and so, more recently, another, simpler, but very effective, method of ink film deposition has been adopted, namely, the use of a K-bar draw-down method. A K-bar is a metal rod which is close-wound in wire of very exact dimensions and, when used to draw down a line of ink deposited at the top of a sample, it produces a wet film with a thickness defined by the thickness of the wire on the K-bar. The K-bar draw-down method is routinely used in the printing ink industry to generate reproducible films so as to allow rapid colour comparisons of ink samples. Figure 5 illustrates the typical components needed to carry out an assessment of the activity of a flat photocatalyst film using a *paii*, namely: a No. 3 K-bar (wet film deposition thickness: 24 microns), an Rz- ink sample, to generate the ink film and a hand-held digital scanner to record the UV-light induced colour changes in the ink film. Figure 5 also shows three samples of Activ™, i.e. without an Rz ink coating (colourless), with a coating (blue) and after UV irradiation of the latter (pink).

Each digital image^{29, 31} of an *paii* ink-coated sample under test, recorded using, say, a scanner, after irradiation time, t , is then analysed using commonly available software so as to determine the average individual RGB values, i.e. $RGB(red)_t$, $RGB(green)_t$, and $RGB(blue)_t$, of the central part of the image of the ink film on the scanned sample. *ImageJ*³³, is an example of free software which is ideal for

performing this analysis, although there are numerous others, including Adobe Photoshop®. Using the $RGB(red)_t$, $RGB(green)_t$, and $RGB(blue)_t$ data thus obtained, a value for R_t , is then calculated, using one of the following expressions:

$$R_t = RGB(red)_t / (RGB(red)_t + RGB(green)_t + RGB(blue)_t) \quad (6)$$

for an Rz or BB66 inks, or

$$R_t = RGB(green)_t / (RGB(red)_t + RGB(green)_t + RGB(blue)_t) \quad (7)$$

for a AV7 ink; details of these other, non-Rz, *paiis* are given below. Thus, R_t is the normalised $RGB(red)$ (when using Rz and BB66 inks, see table 2), or $RGB(green)$ (when using AV7 ink, see table 2), component value, of the RGB digital image of the ink film on the photocatalyst material under test at time t after irradiation. As a consequence, whichever *paii* that is used, every sample of a material tested in this way, yields a series of R_t versus irradiation time, t , values, which, when plotted, yields a curve similar in shape to that illustrated in figure 6 for an Rz-ink coated, Activ™ sample, irradiated with 352 nm UVA light (2 mW cm^{-2}). From the data in this plot, a unique irradiation time, i.e. $ttb(90)$, is then determined, as illustrated in figure 6, where $ttb(90)$ is defined as the irradiation time taken for the ink to undergo 90% of its overall colour change. The value for $ttb(90)$ is usually estimated from the plot of R_t , vs t data and the straight line equation which joins the two data points that straddle the value of $R_t(90)$, see figure 6.

Other work³⁴ shows that, for self-cleaning glass at least, the change in the measured value of $RGB(red)_t$ of an Rz *paii*, at any time, t , during an irradiation, i.e. $\Delta RGB(red)_t$, is related directly to the change in absorbance of the *paii* at 610 nm, as measured using UV/Vis spectrophotometry, i.e. $\Delta Abs_{610}(t)$, which, itself, is a measure of the concentration of Rz in the ink film at time t . This is important in that the rate of change in $\Delta Abs_{610}(t)$, i.e. R_{ink} , a measure of the film's *RP* activity, has been shown to correlate with the rate of destruction of stearic acid ($R_{SA} = d[SA]/dt$) as noted earlier, see figure 4. This suggests that $d(RGB(red)_t)/dt$ is also directly proportional to R_{SA} , and so can also be taken as a measure of the *OP* activity of the film under test, as well as its *RP* activity. Since the kinetics of ink reduction are zero order with respect to dye concentration it follows that the reciprocal of the measured parameter, $ttb(90)$, is proportional to the photocatalytic activity of that sample both for *reductive* and *oxidative* photocatalysed reactions, i.e. reactions (4) and (5), respectively.

3.3 Other *paiis*

As noted earlier, the initial Rz *paii* has been found to be very effective in assessing the photocatalytic activity of materials with *moderate* activities, such as found for most examples of commercial self-cleaning glass, but subsequent work has shown that it performs less well when used on photocatalytic products with activities that are, compared to self-cleaning glass, much higher³⁵ (e.g. StoClimisan Colour paint from Sto AG), or much lower³⁶ (e.g. Hydrotect coated tiles from Deutsches Steinzeug AG). In the course of this work, it was found that two azo dyes, BB66 and AV7,

when used in an otherwise very similar ink formulation and manner to that of an Rz ink, were bleached by the same photocatalytic substrate, respectively, at much faster and slower rates than the Rz ink, see table 2. As a consequence, in recent years the BB66 *paii*^{30, 31} has been used to assess the activity of low activity photocatalytic materials, such as commercial tiles, and the AV7 *paii*^{30, 31} has been used to assess high activity photocatalytic materials, such as commercial photocatalytic paint. Typical R_t versus irradiation time, t , plots generated using these two different *paiis* are illustrated in figure 7, along with digital photographs of the colour changes exhibited by the two different inks during their photocatalysed reduction.

3.4 Round robin tests, repeatability and reproducibility

Repeatability is the degree of agreement between the results of tests, or measurements, on replicate specimens by the same observer in the same laboratory, i.e. *repeatability* is a measure of how well the same experimenter can generate the same results. In contrast, *reproducibility* is usually taken as the ability of an entire experiment to be reproduced by someone, other than the experimenter, working independently. Both *repeatability* and *reproducibility* are usually reported as a standard deviation to an appropriate mean. In order to highlight the *reproducibility* and *repeatability* of the three *paiis* described above and listed in table 2, a series of round-robin tests, involving 5 different test centres, were conducted on commercial samples of self-cleaning glass, paint and tiles, using, respectively, Rz, AV7 and BB66 *paiis*. At each centre, eight samples of each different type of material, (using two 15W 352 nm BLB lights to provide a UVA irradiance of 2 mW cm⁻²) were tested with the appropriate *paii*, each generating a *ttb(90)* value, from which an average value was determined. Details of the average of these averages from all 5 centres, for the each of the three different materials tested, along with the associated average %*repeatability* and %*reproducibility*, are given in table 3.³¹ In general the *repeatability* of the *paii* technology appears acceptable (10-14%), although its *reproducibility* (15-28%) appears, initially, less impressive. But, it worth bearing in mind that the worst of the *reproducibility* results in table 3 was for self-cleaning tiles, for which there is no other accepted test of photocatalytic activity as most examples of photocatalytic tiles are much too low in activity to allow discrimination from a blank sample, when using conventional ISO test methods for example. It follows that no other test exists, apart from *paiis*, that is able to probe the efficacy of such a wide range of materials of very different activities. Finally, it is worth noting that these %*repeatability* and %*reproducibility* values actually compare very favourably to those reported for most of the current ISO photocatalyst activity tests, such as the methylene blue test, ISO 10178:2010, where the results of the inter-laboratory tests revealed a %*repeatability* of 9% and a %*reproducibility* of 31%.^{37, 38}

3.5 Application

Paiis are obviously useful as a qualitative tool to help identify the presence of a photocatalytic coating, or hot spot on an area on a coating, and provide a vivid demonstration of the efficacy of the coating. For example, St. Gobain use it in a

video to demonstrate the efficacy of their self-cleaning glass product, Bioclean™.³⁹ *Pais* can also be used for the quantitative assessment of activity, although this requires the use of a defined UV light source and a well-defined, reproducible coating procedure. Work is currently underway to see if such inks can form the basis of a CEN standard for photocatalyst materials³². One of the more recent innovative uses of *pais* has been in the identification of area of different photocatalytic activity on films produced by combinatorial CVD; the latter technique allows significant variations in thickness, phase and composition to be achieved on a single support substrate in a single coating run, via the variation of the reactant concentrations and reactor conditions; in this work the ink is sprayed onto the photocatalytic film.^{40, 41} Given the simplicity, speed and range of the *paii* technology, it might be expected to feature increasingly in the quality control, marketing and research of photocatalytic materials.

4.0 Sun-burn warning inks

The wavelengths of solar ultraviolet radiation (UVR) that fall on the surface of the Earth lie in the UVB and UVA waveband regions, i.e. 280 – 315 nm and 315 – 400 nm. UVR is a recognised potential health hazard, the most well-known manifestation of which is erythema, i.e. skin reddening or sunburn, which, with further exposure can lead to blistering that is similar to that associated with second-degree burns. Repeated over-exposure to solar UV can ultimately result in premature skin ageing and skin cancer. Skin cancers are classified as either malignant melanoma (MM) or non-melanoma skin cancer (NMSC). According to Cancer Research UK, around 99,500 cases of NMSC are diagnosed each year in the UK; however, since it is readily treatable and frequently cured, it is often omitted from national statistics. In contrast, MM is not easily treated and statistics show that each year in the UK, approximately 13,300 malignant melanoma cases are diagnosed and around 2200 die from the condition. There is also increasing evidence that the human immune system is suppressed due to acute and low-dose UVR exposure, and that this effect is independent of skin type sensitivity.

The amount of solar UV radiation absorbed by the skin at any time is known as the erythemal dose. In quantifying an individual's personal exposure to UVR, the term the '*minimum erythemal dose*' (MED) is often used, where the MED is defined as the minimum amount of radiation likely to cause erythema. The MED for an individual is largely dependent on their skin type, of which there are six (I – VI). For example, for individuals with skin phototype II, which is typical for many Caucasians, the MED is equal to 250 J m^{-2} i.e. 69.4 mW m^{-2} per hour. Since a UV Index value of 1 \equiv 25 mW m^{-2} it follows that even under mild UV solar conditions such as a UVI value of 3 (i.e. 75 mW m^{-2}), as may be observed in April or September in the UK, most Caucasians will sunburn within 1 hour if not properly protected. On a typical summer's day approximately 6% of terrestrial light is UVB and this contributes 80% towards the harmful effects associated with the sun, while the remaining 94% UVA contributes to the remaining 20%.

It follows from the above that there is a clear and growing need for an inexpensive, disposable, personal UV indicator and dosimeter. The former would provide a measure of the real-time, i.e. current, level of ambient UV light, whereas the latter would provide a measure of the total amount of UVR received by a person. The latter is the more important of the two, since in most cases of short UVR exposure times (over 8-12 h) the damage is additive and it is very easy to exceed an MED value of 1, and so be liable to experience sunburn, even when only intermittently exposed to the sun during the day.

There are many, relatively expensive, electronic UVR irradiance monitoring devices, but, apart from their largely prohibitive cost, they are usually also too bulky for practical personal monitoring. There are many UVR *indicators*, most of which are based on photochromic dyes, such as spirobenzopyran⁴² derivatives, that reversibly change structure, and, as a consequence, colour, upon exposure to UVR. Interestingly, there are much fewer examples of commercial UV dosimeter indicators, and those that do exist are usually relatively expensive (typically ca. £1 each) and non-re-usable.

4.1 TiO₂-sensitised UVR indicators and dosimeters based on *RP*

Since most photocatalysts absorb UVR, it is not surprising to note that several,^{7, 43} different, inexpensive and easy to make and use UVR indicator and dosimeter inks have been reported based on *RP*, the key steps of which are summarised in figure 8. Thus, the semiconductor photocatalyst particles absorb *ultrabandgap* light (process I) and the photogenerated electrons and holes are able to, respectively, reduce the redox dye, D_{ox} , i.e. process II_a, and oxidise the SED, process II_b; with process II_a, producing a distinct colour change. In the case of UV indicators based on *RP*, the reduction process is *reversible* and the reduced form of the redox dye is oxygen sensitive (process III), so that, under ambient conditions, the steady-state concentration of D_{ox} , and therefore the colour of the indicator, reflects the current UVR irradiance level to which the indicator is exposed. In the case of UV dosimeters based on *RP* the reduction process is *irreversible* and the reduced form of the redox dye is *not* oxygen-sensitive and reaction III doesn't occur.

An early example⁷ of a *RP* based UV *indicator* employed: P25 TiO₂ (20 mg) as the semiconductor, MB as the redox dye (5 mg) and triethanolamine as the SED (0.1 g). These components are added to 2 g of a 5 wt% dispersion of HEC to produce the ink, which generates clear, dry blue films on glass cover slips by spin coating at 3500 rpm. Upon exposure to UVR, the blue indicator bleaches to a steady-state level of colour which depends upon the UV irradiance level, since in the absence of UVR, the indicator returns to its original blue colour *via* process III in figure 8. A plot of measured %bleaching versus UVA irradiance level (provided by two 8W 368 nm BLB lamps) for the MB/TiO₂/TEOA/HEC UVR indicator is illustrated in figure 9. These results show that such an indicator bleaches when the UVA irradiance is ≥ 3 mW cm⁻², which is useful as it corresponds to a moderate UV exposure level, with a UVI index of ca. 3, that allows a person with skin type II to stay out, unprotected, for

only ca. 1h, without showing signs later in the day of erythema. This UVR indicator has the advantage that it can be made less or more sensitive towards UVR by, respectively, decreasing or increasing the level of TiO_2 used in the ink.

It is possible to change the MB/ TiO_2 /TEOA/HEC UVR indicator into a UVR dosimeter by switching off the reverse process III, see figure 8. This is achieved⁷ by simply placing a UV transparent, gas-diffusion barrier, such as a strip of Sellotape™, between the indicator and the ambient atmosphere. The latter comprises a layer of adhesive on a thin (60 μm) film of regenerated cellulose; a material known for its very low oxygen permeability ($1.6 \times 10^{-16} \text{ cm}^3 \text{ cm cm}^{-2} \text{ s}^{-1} \text{ Pa}^{-1}$)⁸. A plot of the recorded visible spectral changes undergone by the film upon irradiation with UVA light (6.9 mW cm^{-2}) for 15 consecutive exposures of 2 s each, is illustrated in figure 10. Other work showed that the visible spectrum of this dosimeter film remains unchanged for at least 4 h between each exposure, due to the low level of oxygen that permeates through the outer Sellotape™ layer under ambient conditions of temperature and pressure.

In one set of experiments a number of identical Sellotape™/MB/ TiO_2 /TEOA/HEC UV-dosimeter films were exposed to different levels of UVA for the same time and also for different times. The degree of bleaching undergone by each film was then measured spectrophotometrically and these results were then plotted in the form of %bleaching exhibited by the blue-coloured dosimeter versus UV energy, E_{UV} , where E_{UV} is the total energy per cm^2 of the UV light to which the UV-dosimeter film was exposed. The results of this work are illustrated in figure 11 and show a common calibration curve which can be used to assess the total amount of UV exposure of a typical film. The International Commission on Non-Ionising Radiation Protection (ICNIRP)⁵ recommends that the total (unweighted) ultraviolet radiation exposure in the spectral region 315 to 400 nm should not exceed 1000 mJ cm^{-2} . It follows from the data in figure 11 that the UV dosimeter reported, using 20 mg of TiO_2 as the photosensitiser in the film formulation, is too sensitive (by a factor of ca. 5) to act as a UV-exposure indicator, but, this sensitivity can be adjusted to the required level by simply decreasing the amount of TiO_2 in the ink formulation.

4.2 SnO_2 -sensitised UVR dosimeter based on RP

The above UV indicator/dosimeter uses titania particles to absorb the UVR, and because of its bandgap (3.2 eV) this means it will absorb all wavelengths $\leq 380 \text{ nm}$, i.e. both UVA and UVB light. However, as noted earlier, it is mostly the UVB component of solar UV that is responsible for solar-induced biological damage, such as sunburn. As a result, it would seem preferable to use, instead, a semiconductor photocatalyst that has a larger band gap than titania, so that it is effective in absorbing UVB, but not much if any UVA, radiation. In addition, in the previous UV indicator/dosimeter the redox dye was MB, *reversibly* reduced and so able to be readily re-oxidised by ambient oxygen. A more attractive alternative would be a redox dye that is readily and *irreversibly* reduced by the conductance band electrons

generated on the semiconductor photocatalyst particles, since such a feature would avoid the need for an O₂ barrier, such as Sellotape™, and make fabrication of an ink for creating a UVB sensitive dosimeter based on *RP*, a relatively simple process. Thus, in a second generation UV dosimeter⁴³ tin(IV)oxide, SnO₂, was used as the large band-gap, UVB-absorbing semiconductor (3.5 eV) and 2,6-dichloroindophenol (DCIP) as the O₂-insensitive redox indicating dye, which is readily and *irreversibly* reduced by the photogenerated electrons on the SnO₂ particles.

A typical DCIP/SnO₂/glycerol/HEC UVR indicator ink was prepared⁴³ by dissolving 5 g of HEC in 95 ml water at room temperature, followed by stirring for 24 hours. 5 mg of DCIP, 100 mg of nanopowder SnO₂ and 100 mg glycerol were then added to 2 g of the HEC polymer solution. The solution was well stirred to ensure dissolution of the dye and the dispersion of the SnO₂. The indicator was made by spin coating (2400 rpm) a few drops of the ink onto a glass cover slip, to create a blue-coloured film that was as ca. 3.9 microns thick. Upon irradiation with UVB light, the indicator bleached irreversibly, but was not bleached when exposed to the same irradiance (3 mW cm⁻²) of UVA light. A plot of the normalised measured change in absorbance at the $\lambda(\text{max})$ of the DCIP (636 nm) as a function of MED dose, delivered using a solar UV simulator, is illustrated in figure 12 (solid bullet points) and reveals the indicator to be too sensitive to UVR, in that it is fully bleached well before a MED value of 1 (for skin type II) is reached. In order to act as a useful sunburn warning indicator, the colour change should be complete around an MED value of 1, as above this level of UV exposure erythema is increasingly likely. However, as noted earlier, the UVR sensitivity of such indicators can be adjusted by varying the level of the semiconductor photocatalyst present. Thus, in this case, by decreasing the amount of SnO₂ used (from 100 mg to 45 mg) a UVR dosimeter with an appropriate sensitivity as a sunburn warning indicator (for skin type II) was created, as illustrated by the open circle data points in figure 12. As before, this sunburn warning ink functions via *RP*, the key steps of which are summarised in figure 8.

5. Oxygen indicators

Oxygen is a key reactant in a myriad of processes, including animal and plant metabolism and oxidative decay and corrosion. It is no surprise, therefore, to note that there are many areas, particularly in the preservation of materials, where the presence of oxygen is undesirable and its detection and measurement is important. A good example of such an area is modified atmosphere packaging (MAP), as carried out routinely in the food industry, in which the atmosphere above the food is changed during packaging, usually by flushing with an inert gas, such as carbon dioxide or nitrogen, from one that contains 21% oxygen, i.e. air, to one that is largely free of oxygen, i.e. <1-2%. This form of MAP is commonly employed in both the wholesale and retail food packaging industries, since it has been shown to extend the shelf-life of many foods by a factor of, typically, 3-4, when compared to that in air.⁴⁴

Over 60 billion food packages per year are currently MAPed, but this substantial part of the packaging industry suffers a problem in that the monitoring of the integrity of MAP packages is non-trivial and so prevents MAP approaching anything like the desired value of 100% quality assurance for packages in their journey from packager to consumer. Indeed, typically, a packager will sample a MAP line every 300-400 packages and if a fault is found the last set of packaged products are scrapped, the fault fixed and the packaging process restarted. After that, from packager to wholesaler/retailer and then on to consumer, there is little or no further MAP QC. Clearly, a simple, easy, inexpensive method of detecting the presence of oxygen is highly desirable and, as we shall see, *RP* appears able to offer a solution that fills this need.

However, before looking at this solution, it is worth considering what features an ideal oxygen indicator for MAP food packaging should have, namely, it should:

- Be very inexpensive (i.e. ca. 1 p per cm²), so as to not add significantly to the overall cost of the package.
- Be easy to read/interpret, i.e. not require an expensive piece of analytical instrumentation for information extraction, so that an untrained person, without expensive equipment, can check it.
- Comprise non-toxic, non-water-soluble components that have (preferably) food contact approval, since the indicator will be placed inside the food package.
- Have a very long shelf-life under ambient, aerobic conditions. This implies it should only be active as an oxygen indicator when the package has been sealed and is largely or wholly oxygen-free.
- Exhibit an *irreversible* response towards oxygen, since although a *reversible* indicator will indicate the presence of oxygen if a leak develops, it will also return to its original 'no oxygen' state when the oxygen level in the package drops due to the subsequent rapid increase in microbial respiration.
- Be easily and inexpensively integrated into the food packaging process – implying the indicator should be in ink form which can be printed either directly onto the food package or on a label that is easily incorporated in the package.

The above criteria are very demanding and few current smart or intelligent inks come near to addressing them. One notable exception appears to be an indicator made from an oxygen-sensitive, photocatalytic ink based on *RP*.^{8, 45} The ink typically comprises: 5 g of a 5 wt% aqueous dispersion of anatase titania (TiO₂), 1 g of a 5 wt% aqueous solution of MB, 0.3 g of triethanolamine (TEOA) or glycerol, and 20 g of a 5 wt % aqueous solution of HEC. It is, of course, very similar in formulation to that of the MB/TiO₂/TEOA/HEC UVR indicator, although the oxygen sensitive ink has 25% more titania, in order to facilitate its initial activation by a brief exposure to UVR. The mechanism of operation is as outlined in figure 8, with SC = TiO₂, SED = glycerol and D_{ox} = MB. The typical appearance of such an indicator before and after

a brief exposure to UVA radiation (2.5 min, 100W UVA lamp) in air is illustrated in figure 13 and shows that, upon exposure to the UVR, the blue indicator film is rapidly bleached via *RP* (as the MB is reduced to colourless, *leucoMB*, = D_{red} , by the photogenerated electrons, see figure 8, but recovers its colour (in ca. 10 min) under ambient room light conditions. Obviously, in the absence of oxygen, such as in a MAP package, the UV-activated, i.e. photocatalytically-bleached, indicator remains bleached and will only revert back to its original blue colour upon exposure to air. It also follows that this indicator is not an oxygen indicator until and unless it is activated (i.e. photocatalytically bleached) by a brief exposure to UV-light, and so has a very long shelf-life under dark, but otherwise ambient conditions, typically > 1 year.

This type of UV-activated oxygen indicator is *irreversible*, in that it requires UV-activation in order to make it function, and once it has responded to the presence of oxygen and returned to its original colour, this state persists regardless of any subsequent changes in the ambient level of oxygen. It can only be made to function again as an oxygen indicator if it is re-activated by being exposed to a further burst of UVA light. The two features of *irreversibility* and *reusability* are illustrated by the data in figure 14, i.e. a plot of the absorbance of a typical O₂ indicator at 610 nm (where the MB absorbs most strongly) as a function of time under ambient conditions, with each arrow indicating a short exposure (2 min, 100 W UVA lamp) to UVA light, which activates the indicator by bleaching the dye. It can be shown⁴⁴ that, after activation,⁴⁵ the initial rate of colour recovery exhibited by this indicator is directly proportional to the ambient level of oxygen.

The novel features of this smart oxygen-sensitive ink/indicator include: (i) UVA activated, (ii) irreversible, (iii) re-useable, (iv) easily handled, (v) non-toxic, (vi) very inexpensive, (vii) printable and (viii) a long shelf-life. The technology was used by the Finnish-based label manufacturer, UPM Raflatac Ltd.⁴⁶ to create a UV-activated, oxygen sensitive label to identify leaking MAP food packages. Subsequent work, using colloidal TiO₂, showed that the ink could be printed onto plastic film using an ink-jet printer.⁴⁷

More recently, UV-activated, oxygen-sensitive pigment particles, based on the same process as illustrated in figure 8 have been produced,⁴⁸ and a schematic illustration of their construction is given in figure 15(a). When extruded with low density polyethylene, a UV-activated, oxygen sensitive plastic film is created, as illustrated in figure 15(b). As before, after UVA-activation, the O₂ smart plastic film will only return to its original blue colour if an oxidising gas, such as O₂ is present, in which the colour recovery is described by step (III) in Fig. 8, or, more specifically:



In contrast to the relatively fast photoactivation step (< 90 s at UVA irradiance of 4 mWcm⁻²), the dark recovery step, back to the O₂ smart plastic film's initial blue

colour, takes ~2.5 days in air under ambient conditions (~21°C, ~65% RH), see solid squares in figure 16, a plot of the CIELAB colour measuring parameter, Δb^* , as measured using diffuse reflectance spectroscopy, for a typical O₂ smart plastic film after UV activation (bleaching), as a function of time in ambient air. This recovery time is significantly slower than that observed for a water-based O₂-indicating ink, which recovers in ~10-20 min, see figure 14. From the results of other work⁴⁹, also involving reaction (8) in a hydrophobic medium, it is suggested that this lengthy recovery time is due, at least in part, to the formation of the charged species, MB (which is cationic) and OH⁻, as seen in equation (8), being hindered by the more hydrophobic film medium (in this case LDPE) compared to the more hydrophilic medium of a water-based ink film. In a fridge, set at 5°C, the recovery of the colour of the O₂ sensitive, indicator plastic film is much slower, see open square data points in figure 16, taking typically 6 days to fully recover its original colour, although most of the colour has returned after a period of 4 days. This feature has prompted the suggestion that such an indicator film could be used to indicate how long an opened package, has been left in the fridge, i.e. effectively a 'consume within' indicator. The commercial potential of these films in this role is currently being explored.

6. Metal oxide removal

Metal corrosion in general, and stainless steel corrosion in particular, is a major concern to many industries (e.g. energy, construction and chemical) and attempts to address the issue are estimated to cost the UK around 4% of GNP per annum. Most metals are thermodynamically unstable in air and aqueous solution, and so owe their durability to the formation of passive, albeit often thin (< 2 nm), surface metal oxides. However, if/when they thicken, due to further oxidation of the underlying metal, these metal oxides can become contaminated with undesirable corrosion products and eventually flake off; as a result, in many cases they need to be removed. Strong acids or chelating agents are normally used to effect this process but other reducing agents have also been employed^{49,50}. An example of the latter is the use of low oxidation metal ions (the LOMI process) which has been used to clean up contaminated metal pipework in nuclear plant coolant systems. Typically, a LOMI treatment employs a vanadium (II) complex as a one electron agent for reducing the solid iron (III) contaminated oxide layer that forms on stainless steel, to its more soluble iron (II) form.^{50, 51}

Work carried out by many groups have demonstrated that if TiO₂ particles in aqueous solution are irradiated in the absence of oxygen, but in the presence of an SED to mop up the photogenerated holes, then the photogenerated electrons accumulate on the TiO₂ particles, eventually turning them blue, due to Ti(III) formation.²⁰ It follows that it might be possible to make a photocatalyst ink, comprising photocatalytic TiO₂ particles and an SED, that when coated on a thick oxide film covered sample of a metal, such as steel, that the photogenerated electrons may be able to reduce the oxide back to its metallic form, as illustrated by the schematic in figure 17. Such an anti-tarnish photocatalytic ink is an example of

RP. With this object in mind,⁹ an anatase titania-based, metal tarnish-removing ink was created by mixing 200 mg of PC500, an anatase TiO₂ powder (Millenium Inorganic Chemicals; specific surface area 350 m² g⁻¹; particle size ca. 4 nm), with 2 g of 1.5% HEC aqueous solution into which 250 mg of glycerol (the SED) had been added. The ink was then applied, via a doctor blade technique, onto a 'bronze' coloured, tarnished surface of a stainless steel coupon and left to dry, as a 20 micron thick, white film. The bronze, tarnished stainless steel sample (AISI 316) was prepared by annealing it in air at 450°C for 30 min, XPS analysis of which suggests⁹ the 'bronze' oxide coating (ca. 15 nm thick) to be mainly Fe₂O₃.

Photographs A and B in figure 18 are those of the bronze stainless steel sample before and after coating with the photocatalyst-based tarnish removing ink. The latter was then irradiated with UV light, for 15 min, through a brass 'TiO₂' template (C), and the ink then washed off using water to reveal an image of the 'TiO₂' template on the coupon, (D), in which the bronze coloured oxide coating has been removed by the illuminated parts of the ink. The UV illumination of the ink was carried out using a 200 W Xe/Hg Oriel lamp, delivering ca. 20 mW/cm² at 365 ± 20 nm UVA light. The TiO₂/glycerol/HEC ink was also able to effect the removal of the bronze oxide tarnish produced on other steels (such as AISI 302, 304, 347), by the same heat-treatment process. It was also effective in cleaning tarnished silver, such as a black Ag₂S layer on a silver metal coupon, generated by exposing the silver coupon to H₂S. Thermodynamically, the tarnish-removing process should work for all metal oxides/sulfides which have redox potentials > the redox potential of the conductance band electrons (E^o = -0.2 V vs SHE for anatase TiO₂). The potential scope of this easy to apply, UV-driven, anatase TiO₂-based photocatalytic ink, which works via *RP*, for regenerating tarnished metal surfaces under ambient conditions is significant, since it is inexpensive, simple, effective, controllable and avoids the use of aggressive chemical reagents.

7. Conclusions

Reductive photocatalysis is a less well-studied, but significant part of semiconductor photocatalysis, in which a key feature is the irreversible photo-oxidation of a sacrificial electron donor, such as an alcohol, EDTA or cysteine. Mostly known for the photoreduction of metal ions and of water, recent work in this area has focussed on the use of *RP* in smart inks, i.e. inks that provide useful analytical information or serve a useful active function. Developed smart inks based on *RP* inks include those for: (i) identifying the presence of and assessing the activity of photocatalytic materials with a wide range of activities and forms, (ii) indicating the level and dose of solar UV that is responsible for sunburn, (iii) indicating the presence and level of O₂ (and which can be activated using UV light) for use in the food packaging industry and (iv) removing metal tarnish. There appears to be a good level of commercial interest in the above products, which might merit greater research into the general area of *RP*. There are some obvious very tough processes *RP* might be able to facilitate, such as the *efficient* photocatalysed reduction of CO₂ and N₂, which even if

achieved using an SED, would represent a significant breakthrough in solar energy research. Possibly less difficult reactions, but not without difficulty, include the reduction/detection of: NO_x , CO and unsaturated organics; all of which are likely to have commercial impact, if achieved efficiently and cheaply. For example, with regard to the latter process, if *RP* could be used to create a robust, inexpensive, reproducible indicator of the growth hormone ethylene, this would most likely find application as a ripeness indicator. The latter has the potential to transform how we currently handle, amongst other things, all fruit, from farm to the consumer. Overall, the area of *RP* and smart inks is an emerging area of promise that is worth watching, if not exploring.

References

1. M. Pera-Titus, V. Garcia-Molina, M. A. Banos, J. Gimenez and S. Esplugas, *Appl. Catal. , B*, 2004, **47**, 219-256.
2. H. Wang, L. Zhang, Z. Chen, J. Hu, S. Li, Z. Wang, J. Liu and X. Wang, *Chem. Soc. Rev.*, 2014, **43**, 5234-5244.
3. M. R. Hoffmann, S. T. Martin, W. Choi and D. W. Bahnemann, *Chem. Rev.*, 1995, **95**, 69-96.
4. N. Serpone, E. Pelizzetti and Editors, 1989, 650.
5. J. L. Muzyka and M. A. Fox, *J. Photochem. Photobiol., A: Chem.*, 1991, **57**, 27-39.
6. http://en.wikipedia.org/wiki/Photocatalyst_activity_indicator_inks, Last Accessed: August 2014.
7. A. Mills, S. Lee and M. Sheridan, *Analyst*, 2005, **130**, 1046-1051.
8. S. Lee, A. Mills and A. Lepre, *Chem. Commun.*, 2004, 1912-1913.
9. A. Mills and D. Hazafy, *Chem. Commun.*, 2012, **48**, 525-527.
10. A. Mills, R. H. Davies and D. Worsley, *Chem. Soc. Rev.*, 1993, **22**, 417-425.
11. A. Mills and S. Lee, *J. Photochem. Photobiol., A: Chem.*, 2002, **152**, 233-247.
12. K. Rajeshwar, *J. Appl. Electrochem.*, 2007, **37**, 765-787.
13. M. I. Litter, *Appl. Catal. , B*, 1999, **23**, 89-114.
14. S. - . Lee and A. Mill's, *Platinum Met. Rev.*, 2003, **47**, 61-72.
15. A. Mills, *Insights Spec. Inorg. Chem.*, 1995, , 457-485.
16. E. Borgarello, R. Harris and N. Serpone, *Nouv. J. Chim.*, 1985, **9**, 743-747.
17. A. Mills and G. Porter, *J. Chem. Soc. , Faraday Trans. 1*, 1982, **78**, 3659-3669.
18. E. Borgarello, N. Serpone, G. Emo, R. Harris, E. Pelizzetti and C. Minero, *Inorg. Chem.*, 1986, **25**, 4499-4503.
19. A. Mills and J. Wang, *J. Photochem. Photobiol., A: Chem.*, 1999, **127**, 123-134.
20. N. Serpone, I. Texier, A. V. Emeline, P. Pichat, H. Hidaka and J. Zhao, *J. Photochem. Photobiol., A: Chem.*, 2000, **136**, 145-155.
21. M. Anpo, N. Aikawa and Y. Kubokawa, *J. Phys. Chem.*, 1984, **88**, 3998-4000.

22. F. Mahdavi, T. C. Bruton and Y. Li, *J. Org. Chem.*, 1993, **58**, 744-746.
23. <http://www.inkintelligent.com/>, Last Accessed: August 2014.
24. V. Augugliaro, V. Loddo, G. Palmisano and L. Palmisano, 2010, pp. 267.
25. A. Mills, A. Lepre, N. Elliott, S. Bhopal, I. P. Parkin and S. A. O'Neill, *J. Photochem. Photobiol., A: Chem.*, 2003, **160**, 213-224.
26. A. Hagfeldt and M. Graetzel, *Chem. Rev.*, 1995, **95**, 49-68.
27. A. Kafizas, *Private Correspondance*, 2014, .
28. A. Mills, J. Wang, S. Lee and M. Simonsen, *Chem. Commun.*, 2005, , 2721-2723.
29. A. Mills, J. Hepburn, D. Hazafy, C. O'Rourke, J. Krysa, M. Baudys, M. Zlamal, H. Bartkova, C. E. Hill, K. R. Winn, M. E. Simonsen, E. G. Soegaard, S. C. Pillai, N. S. Leyland, R. Fagan, F. Neumann, C. Lampe and T. Graumann, *J. Photochem. Photobiol., A: Chem.*, 2013, **272**, 18-20.
30. A. Mills, C. O'Rourke, K. Lawrie and S. Elouali, *ACS Appl. Mater. Interfaces*, 2014, **6**, 545-552.
31. A. Mills, J. Hepburn, D. Hazafy, C. O'Rourke, N. Wells, J. Krysa, M. Baudys, M. Zlamal, H. Bartkova, C. E. Hill, K. R. Winn, M. E. Simonsen, E. G. Soegaard, S. Banerjee, R. Fagan and S. C. Pillai, *J. Photochem. Photobiol., A: Chem.*, 2014, **290**, 63-71.
32. K. Nakata and A. Fujishima, *J. Photochem. Photobiol., C: Photocat. Rev.*, 2012, **13**, 169-189.
33. <http://rsb.info.nih.gov/ij/download.html>, Last Accessed: August 2014.
34. A. Mills, N. Wells and C. O'Rourke, *Catal. Today*, 2014, **230**, 245-249.
35. http://www.climasan.com/33245_EN-Climasan.com.htm, Last Accessed: August 2014.
36. http://www.deutsche-steinzeug.de/en/news/presse_und_news_detail.html?nd_ref=2586, Last Accessed: August 2014.
37. ISO 10678: 2010, 'Fine ceramics, advanced technical ceramics) –Determination of photocatalytic activity of surfaces in an aqueous medium by degradation of methylene blue', ISO, Geneva, 2010.
38. A. Mills, C. Hill and P. K. J. Robertson, *J. Photochem. Photobiol., A: Chem.*, 2012, **237**, 7-23.

39. <http://webtv.picardie.fr/video621>, Last Accessed: August 2014.
40. A. Kafizas, C. Crick and I. P. Parkin, *J. Photochem. Photobiol., A: Chem.*, 2010, **216**, 156-166.
41. A. Kafizas, A. Mills and I. P. Parkin, *Anal. Chim. Acta*, 2010, **663**, 69-76.
42. T. M. Trumble, US Pat., 3787687, 1974.
43. A. Mills and P. Grosshans, *Analyst*, 2009, **134**, 845-850.
44. A. Mills, *Chem. Soc. Rev.*, 2005, **34**, 1003-1011.
45. S. Lee, M. Sheridan and A. Mills, *Chem. Mater.*, 2005, **17**, 2744-2751.
46. Anon, in *in Active and Intelligent Pack News*, ed. nymous PIRA International Ltd., Leatherhead, 2006, pp.2-3.
47. K. Lawrie, A. Mills and D. Hazafy, *Sens. Actuators, B*, 2013, **176**, 1154-1159.
48. A. Mills and A. Graham, *Analyst*, 2013, **138**, 6488-6493.
49. A. Mills and K. Lawrie, *Sens. Actuators, B*, 2011, **157**, 600-605.
50. M. G. Segal and R. M. Sellers, *J. Chem. Soc., Chem. Commun.*, 1980, , 991-993.
51. V. Balaji, V. S. Tripathi, S. J. Keny and G. Venkateswaran, *Ind. Eng. Chem. Res.*, 2006, **45**, 4461-4470.

Table 1: Early examples of Reductive Photocatalysis

Reduction	SED	SC	ref
Water and the hydrogen evolution reaction (HER)	EDTA	Pt/TiO ₂	20
Metal ion reduction/deposition	MeOH	Pt, Au, and Rh	21
Reversible bleaching of methylene blue	MeOH	TiO ₂	22
Dechlorination of chlorophenols	EDTA	TiO ₂	23
Hydrogenation of alkenes and alkynes to alkanes	H ₂ O	TiO ₂ and Pt/TiO ₂	24
Reduction of nitrophenol to aminophenol	EtOH	TiO ₂	25

Table 2: Structures, spectral characteristics and comments on key redox dyes used in *Paiis*

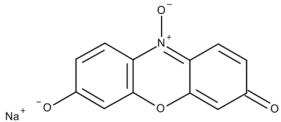
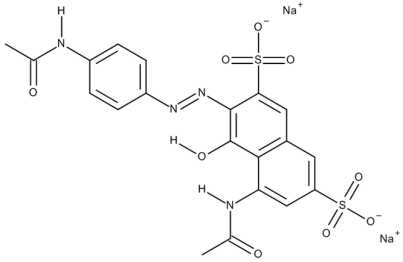
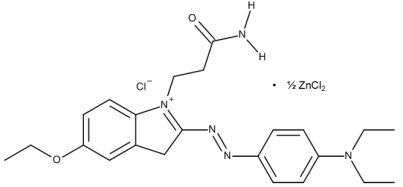
Dye	Redox Indicator Dye (D_{ox})	$\lambda_{max} (D_{ox}) / nm$		Colour of Ink before (and after) SP bleaching	Comments (UVA light source: 15W 368 nm BLB)
		In solvent	In dried ink		
Rz		598 (H ₂ O)	608	Blue (Pink)	The first reported ⁶ <i>paii</i> with <i>tbt</i> values of 0.8 and 30 min recorded when used on a thick (ca. 2 microns) sol gel and Activ™ TiO ₂ coated glass films, using UVA irradiances of 0.15 and 1.65 mW cm ⁻² , respectively. Best suited for medium activity photocatalytic materials, such as self-cleaning glass.
AV7		525 (H ₂ O)	520	Pink (Colourless)	A much more difficult to reduce dye than Rz and so ideal for testing on high activity materials, like self-cleaning paint and thick TiO ₂ sol gel films ³¹ . <i>Tbt</i> values of 0.3 and >120 min when used on a sol gel and Activ™ TiO ₂ coated glass films using a UVA irradiance of 1.65 mW cm ⁻² .
BB66		615 (H ₂ O)	582	Blue (Colourless)	A much easier to reduce dye than Rz and so ideal for testing on low activity materials, like self-cleaning (Hydrotect®) tiles. <i>Tbt</i> values of 0.3 and 10 min recorded when used on a sol gel and Activ™ TiO ₂ coated glass films, using UVA irradiances of 0.15 and 1.65 mW cm ⁻² , respectively.

Table 3: Summary of *Paii* Round Robin Results*

<i>Paii</i> (test sample)	Average (of Averages)** <i>ttb(90)</i>/s	Repeatability (%)	Reproducibility (%)
Rz (Pilkington Activ™ glass)	226	13	15
AV7 (StoClimasan paint)	267	10	21
BB66 (Hydrotect tiles)	458	14	28

*: irradiance: 2 mW cm⁻² 352 nm UVA irradiation from two 15W BLB lamps; 5 centres in round robin, 8 specimens of each sample type analysed by each and every centre.

**For each sample type tested, each and every centre generated an average *ttb(90)* value and the averages of these averages are reported here.

Figure Legends

(1) Schematic illustration of the basic principles of semiconductor photocatalysis. Involving: (I) absorption of radiation of energy greater or equal to the band gap, E_{bg} , of the semiconductor, SC, thereby generating an electron-hole pair; (IIa) migration of photogenerated conduction band electrons, e^- , to the surface and reaction with an adsorbed electron acceptor, **A**; (IIb) migration of photogenerated valence band holes, h^+ , to the surface and reaction with an adsorbed electron donor, **D**; (III) electron-hole recombination. The combination of processes IIa and IIb are responsible for the photocatalytic process.

(2) Schematic illustration of the processes that occur in a photocatalyst activity indicator ink, i.e. *paii*, containing a sacrificial electron donor (**SED**), such as glycerol, and a redox indicating dye, **D_{ox}**, coated onto a film of a semiconductor photocatalyst. Upon absorption of light $\geq E_{bg}$ by the SC, many of the photogenerated h^+ 's will oxidise irreversibly the **SED**, leaving an identical number of photogenerated e^- 's to reduce irreversibly either ambient oxygen or the redox dye, **D_{ox}**, to produce **D_{red}**. The latter reaction is favoured because of the high concentration of **D_{ox}** and low solubility of oxygen in the ink.

(3) Sequence of photographs of a typical Rz *paii* ink coated onto a sample of plain glass (right hand side) and a commercial sample of self-cleaning glass Activ™ (left hand side) recorded as a function of irradiation time (UVA irradiance = 12.4 mW cm⁻²); the UVA exposure times were, clockwise starting from the left hand side, 0, 1, 2 and 3 min, respectively.

(4) Measured²⁹ initial rate of change in absorbance (at 585 nm) of a typical Rz *paii* ink (R_{ink}) vs. the measured rate of removal of a stearic acid film – measured using FTIR via the area of the stearic acid peaks over the range 2700-3000 cm⁻¹ (R_{SA}) - for a series of TiO₂-coated glass samples of different photocatalytic activity. UVA irradiance provided by a two 8W blacklight blue lamps with a combined irradiance of 0.32 mW cm⁻²;

(5) Typical components needed to carry out an assessment of the activity of a flat photocatalyst film using a *paii*, namely: an Rz- ink sample, to be used with a No. 3 K-bar, to deposit a wet ink film of 24 microns, and a hand-held digital scanner to record the UV-light induced colour changes in the air-dried (60 min) ink film. At the bottom left hand side of the figure are three different samples of Activ™, namely, from left to right): without an Rz ink coating, with a coating (blue) and after UV irradiation of the latter (pink).

(6) Illustrative plot of a typical set of data, based on the RGB analysis of the digital photographs shown above the plot of R_t vs t for an Rz ink on a sample of self-cleaning glass, highlighting the simple least-squares method of determining $ttb(90)$ based on a calculated value of $R_t(90)$ ($= 0.9\Delta R(total) + R(min)$)³². The UVA irradiance was 2 mW cm⁻².

(7) Typical set of data, based on the RGB analysis of the digital photographs shown above the plot of R_t vs t , for (●) an AV7 ink on a sample of self-cleaning paint, and (○) a BB66 ink on a sample of a self-cleaning tile. In both cases, the red

square corresponds to the point when $t_{tb}(90)$ is reached. The UVA irradiance was 2 mW cm^{-2} .

(8) Schematic of the key processes in a SC-based UV indicator/dosimeter, comprising: (I) the absorption of *ultrabandgap* light by the SC, to generate electron, hole pairs, $\text{SC}(\text{h}^+, \text{e}^-)$; (IIa) subsequent reaction of some of the photogenerated electrons with the redox dye, D_{ox} , to form D_{red} ; where the latter two species are very differently coloured; (IIb) irreversible oxidation of a SED , to form SED_{ox} ; (III) D_{red} is re-oxidised to D_{ox} by ambient oxygen; note this last step pertains ONLY to a UVR SC-based indicator (or O_2 -indicator, *vide infra*).

(9) Measured %bleaching versus UVA irradiance level (provided by two 8W 368 nm BLB lamps) for the MB/TiO₂/TEOA/HEC UVR indicator, with illustrative photographs of the indicator in its coloured (no UV) and subsequently fully bleached (high UVR irradiance) states⁸.

(10) Recorded (top to bottom) visible spectral changes exhibited by a MB/TiO₂/TEOA/HEC UVR indicator film, with a Sellotape™ covering, upon irradiation with UVA light (6.9 mW cm^{-2}) for 15 consecutive exposures of 2 s each⁸.

(11) Measured %bleaching for a MB/TiO₂/TEOA/HEC/ Sellotape™ UVR dosimeter versus UVA energy exposure level, E_{UV} .⁸

(12) Normalised, measured⁴² change in absorbance, at 610 nm, in a DCIP/SnO₂/glycerol/HEC/ UVR dosimeter when exposed to simulated solar UV light for different periods of time, so as to correspond to solar UV doses that are equivalent to MED levels for skin type II that span the range 0 to 1 MED. The solid points correspond to those recorded for a typical DCIP ink, which used 100 mg SnO₂ in its formulation. The open circles were generated using an otherwise the same ink formulation, but with less (45 mg) SnO₂. The solar UV simulator utilised the light from a 150 W Xe lamp, filtered through UG5 and WG320 Schott optical filters.

(13) Typical photographed appearances of MB/TiO₂/glycerol/HEC, UV activated, O_2 indicator before and after a brief exposure to UVA radiation (2.5 min, 100W UVA lamp) in air^{9,43}. This work reveals that, upon exposure to the UVR, the blue indicator film is rapidly bleached via *RP*, as the original MB is reduced to *leuco*-MB, = D_{red} , by the photogenerated electrons, see figure 8, but recovers its colour (in ca. 10 min) under ambient room light conditions.

(14) Absorbance (610 nm) versus time profile for a typical MB/TiO₂/TEOA/HEC indicator film upon repeated exposure (indicated by ↓) to 2 min of UVA light (100 W BLB) under ambient aerobic conditions⁹.

(15) (a) cross-sectional schematic illustration of the nano-particulate pigment particles, used to create O_2 -sensitive LDPE-based plastic films, before (blue) and after (white) UVA activation and (b) photographs of the O_2 -sensitive LDPE-based MB/glycerol/TiO₂ pigmented extruded plastic films, before and after exposure (90 s) to 4 mW cm^{-2} UVA radiation.⁴⁷

(16) Measured variations of the b^* parameter of the CIELAB colour measurement system as a function of time in the dark for a UV activated LDPE-based

MB/glycerol/TiO₂ pigmented extruded plastic film stored in a fridge at 5°C (solid squares) or at ambient temperature (21°C), open squares.⁴⁷

(17) Schematic illustration of the key processes involving the removal of a metal oxide (MO) film on a metal (M) using a UV-driven TiO₂ photocatalyst ink containing a SED, such as glycerol.¹⁰

(18) Photographs of an annealed stainless steel coupon without (**A**) and with (**B**) a rectangle of the TiO₂/glycerol/HEC tarnish removing ink cast on its surface. Irradiation of **B** with UVA light (20 mW cm⁻²), through a brass 'TiO₂' template (**C**), following by rinsing off the ink revealed an image of the 'TiO₂' template on the coupon, (**D**), in which the bronze coloured oxide coating has been removed by the illuminated section of the ink.¹⁰

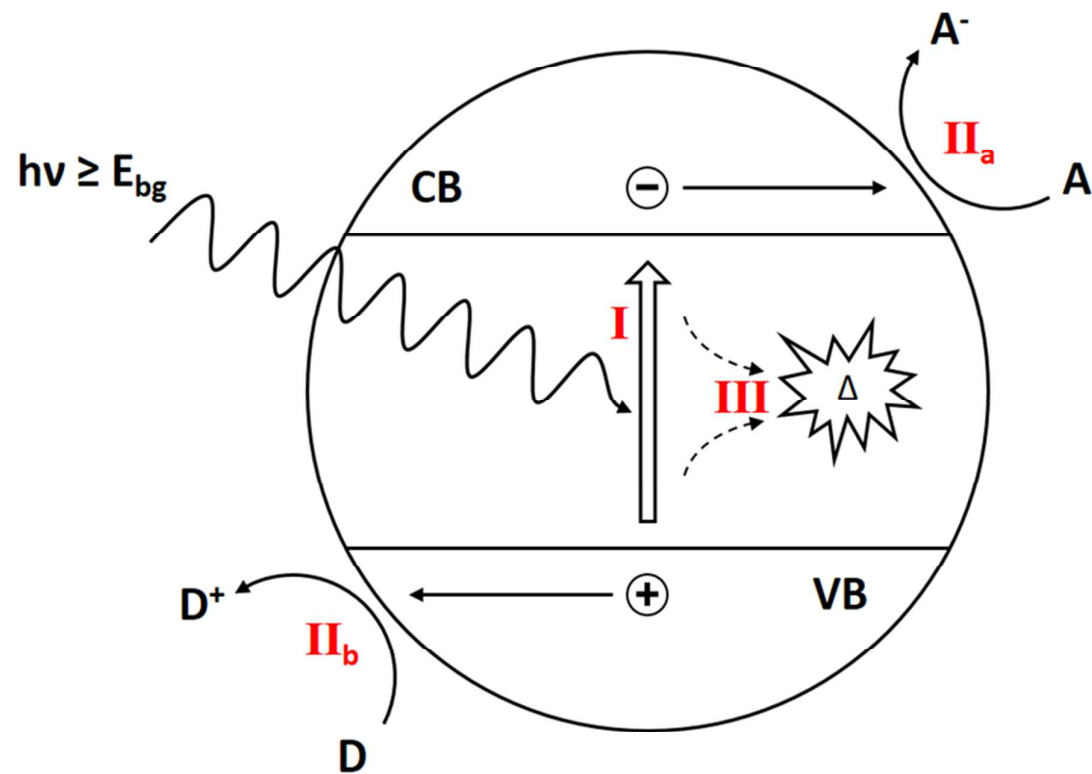


Fig. 1

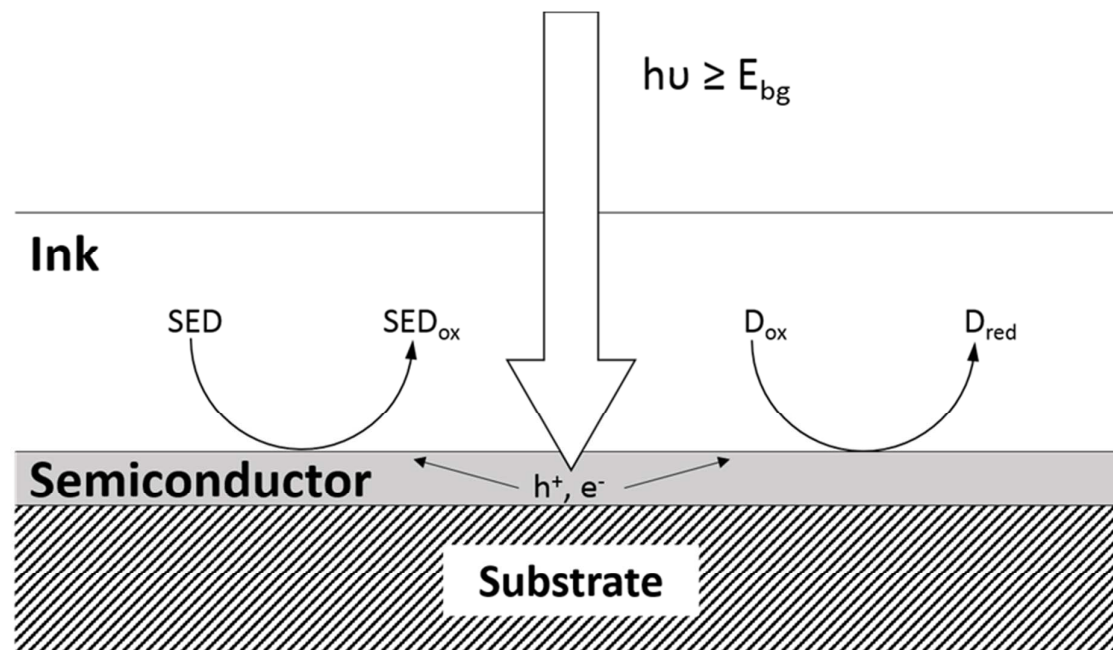


Fig. 2

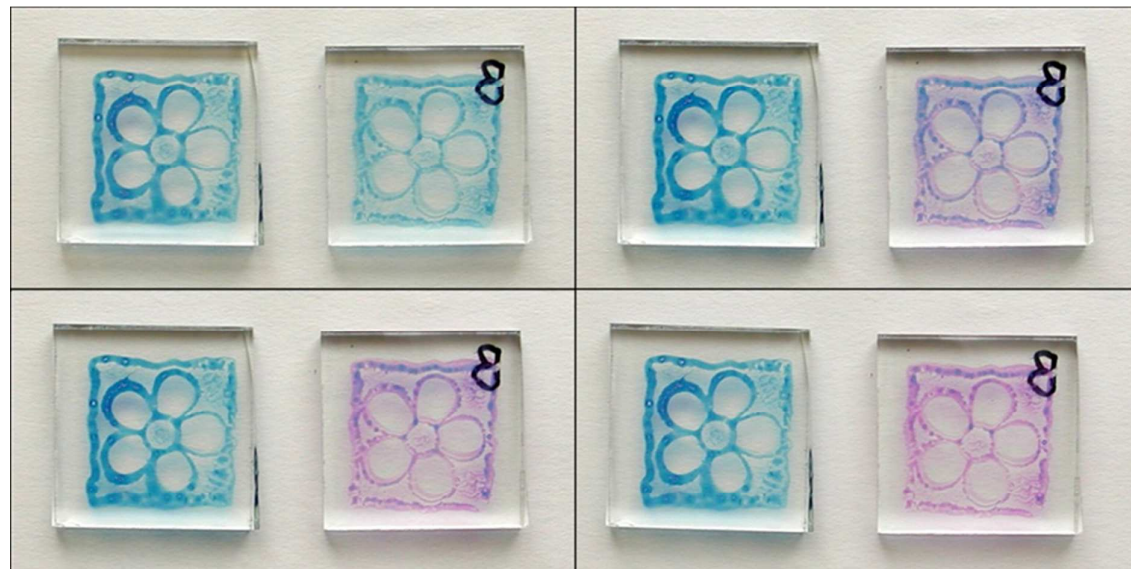


Fig. 3

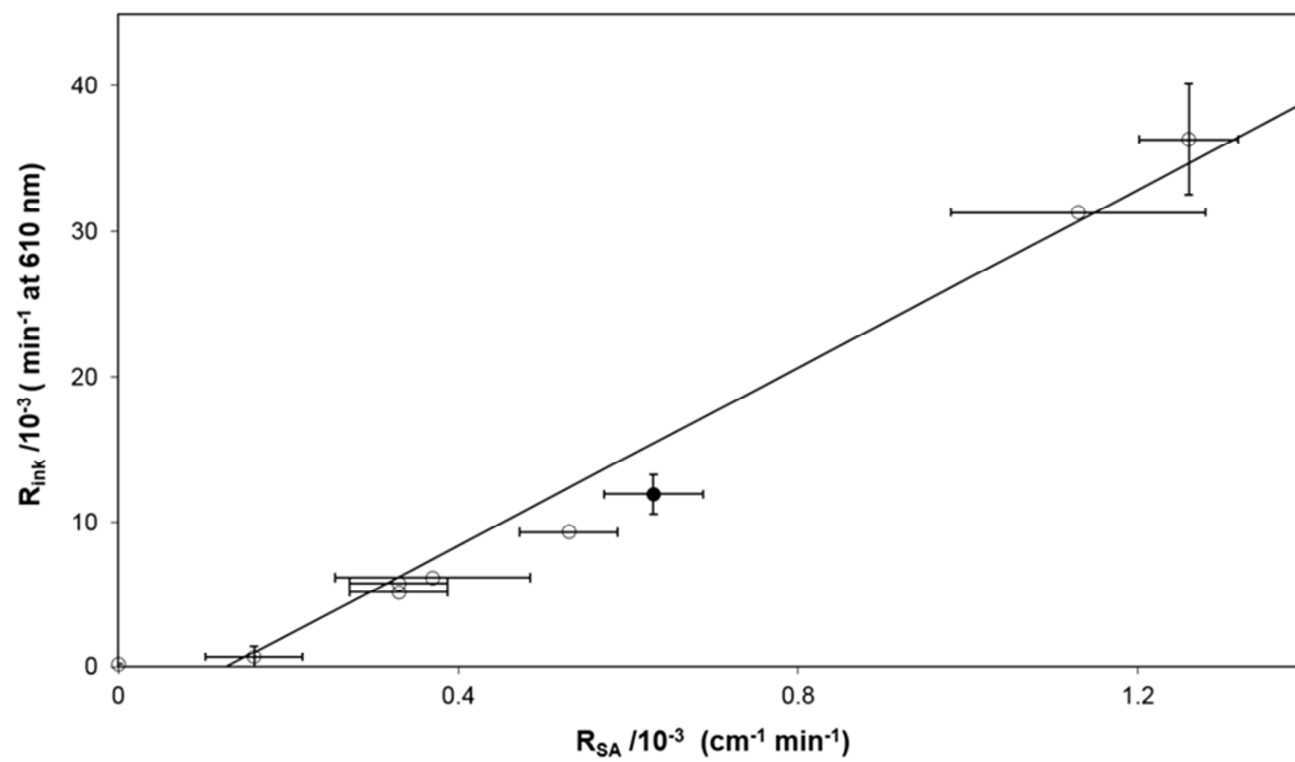


Fig. 4



33

Fig. 5

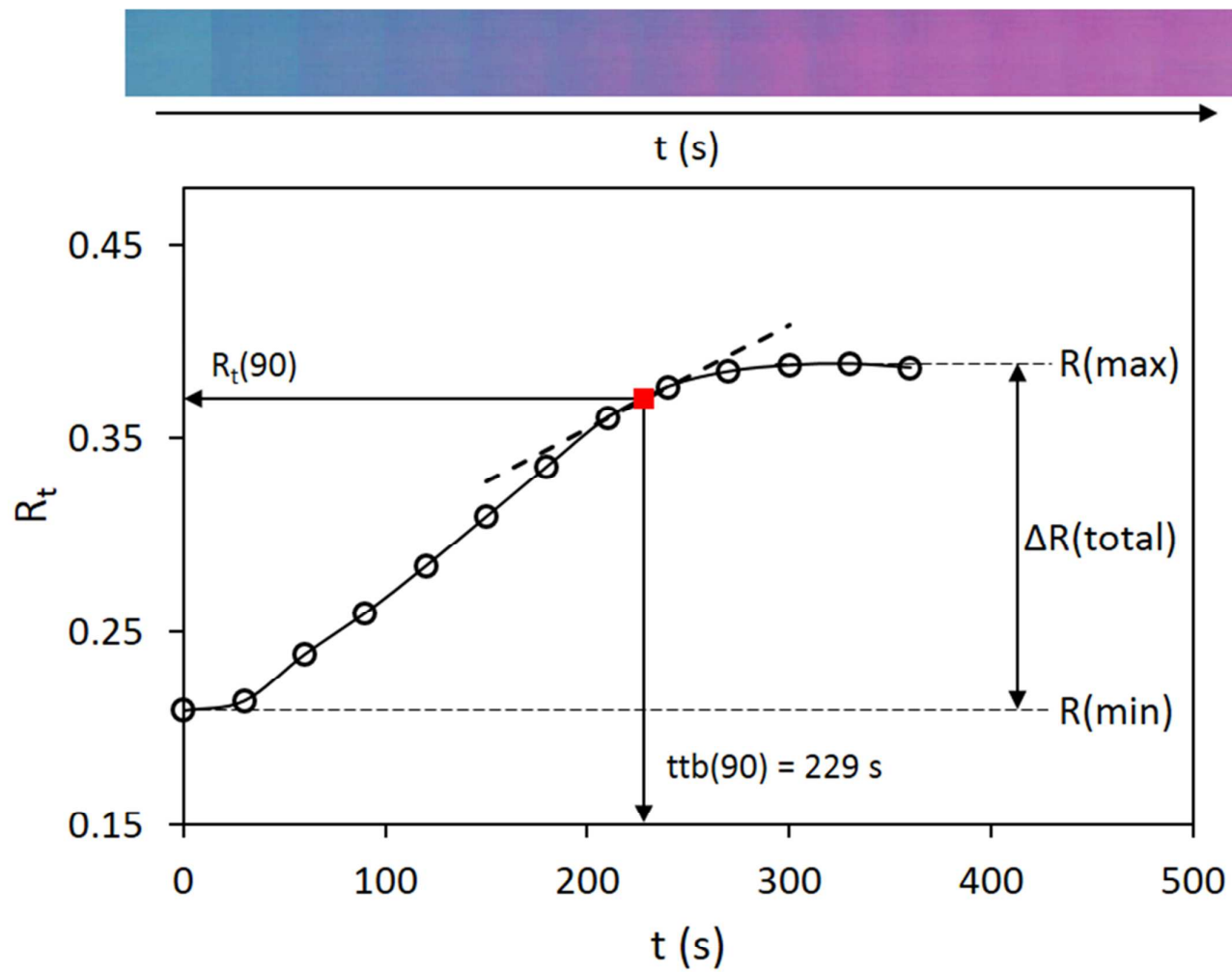


Fig. 6

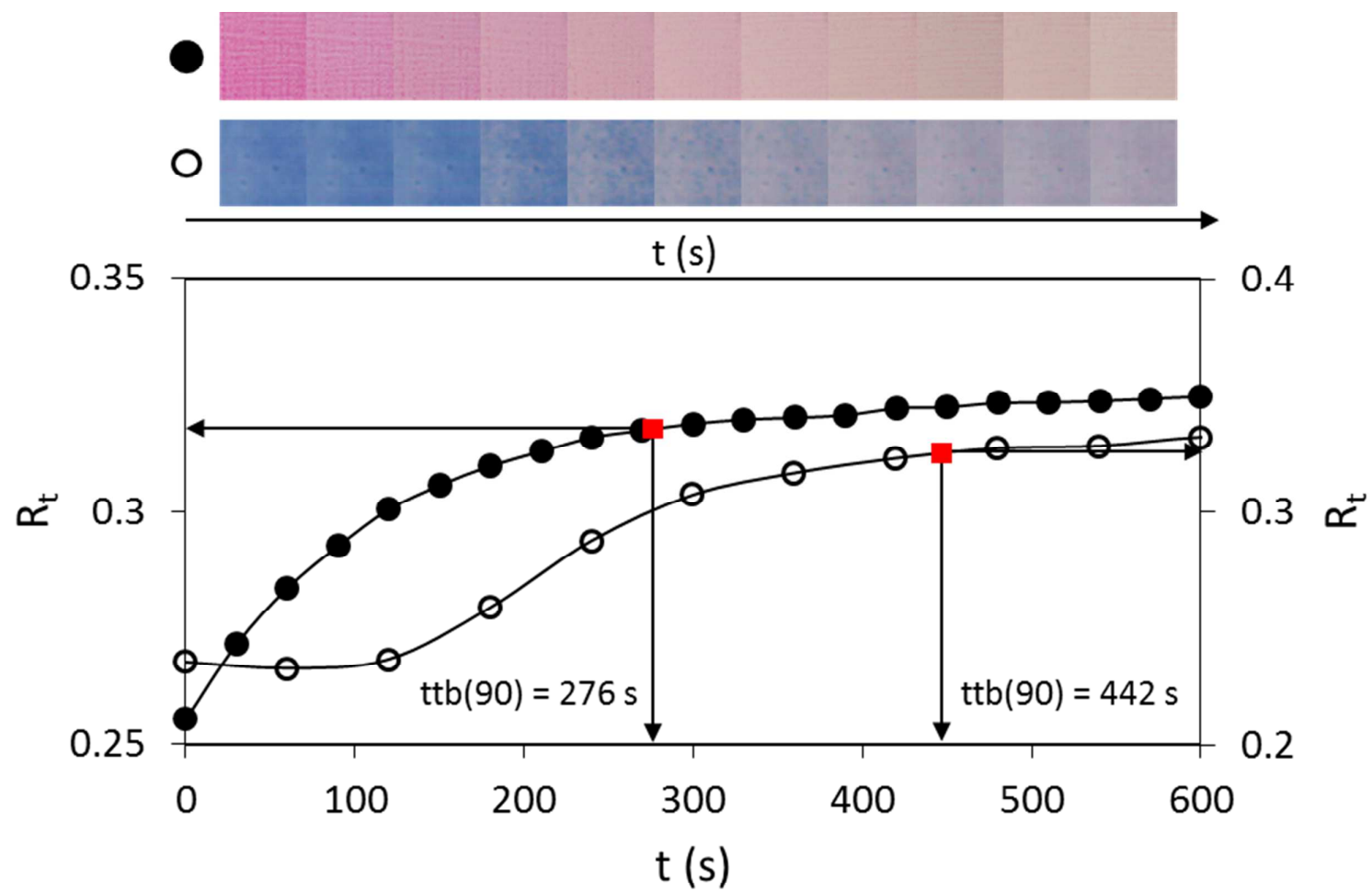


Fig. 7

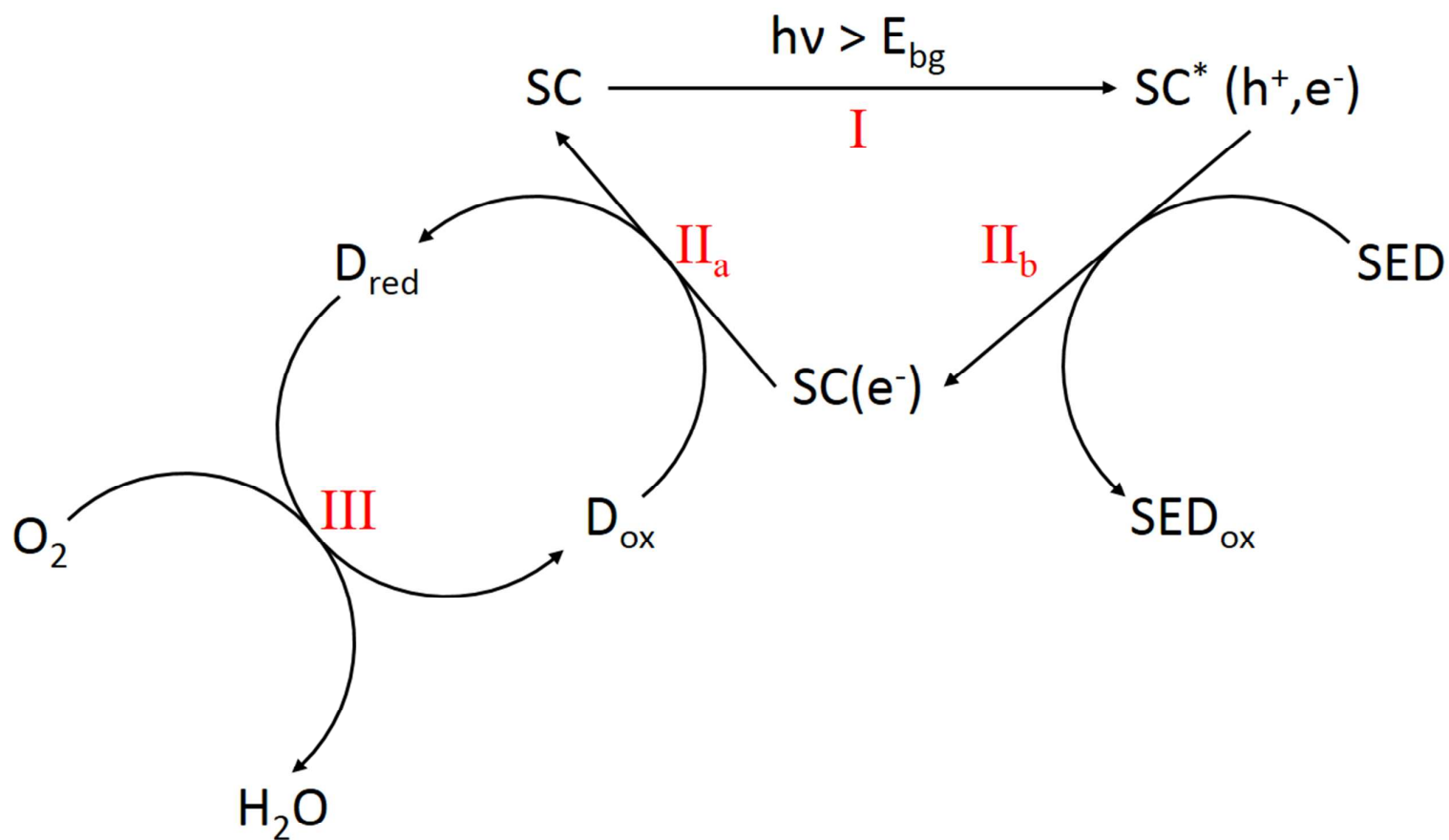
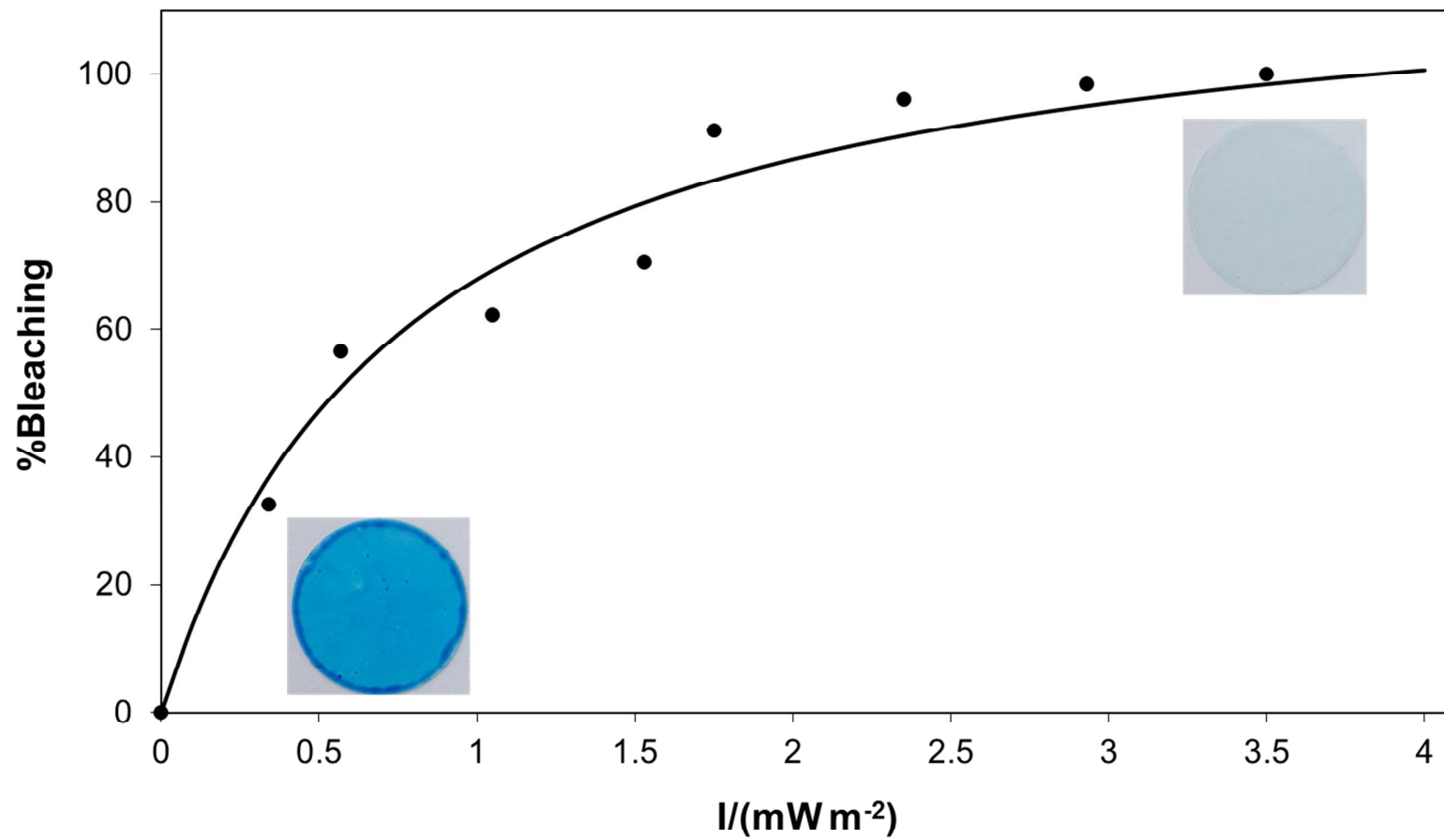


Fig. 8



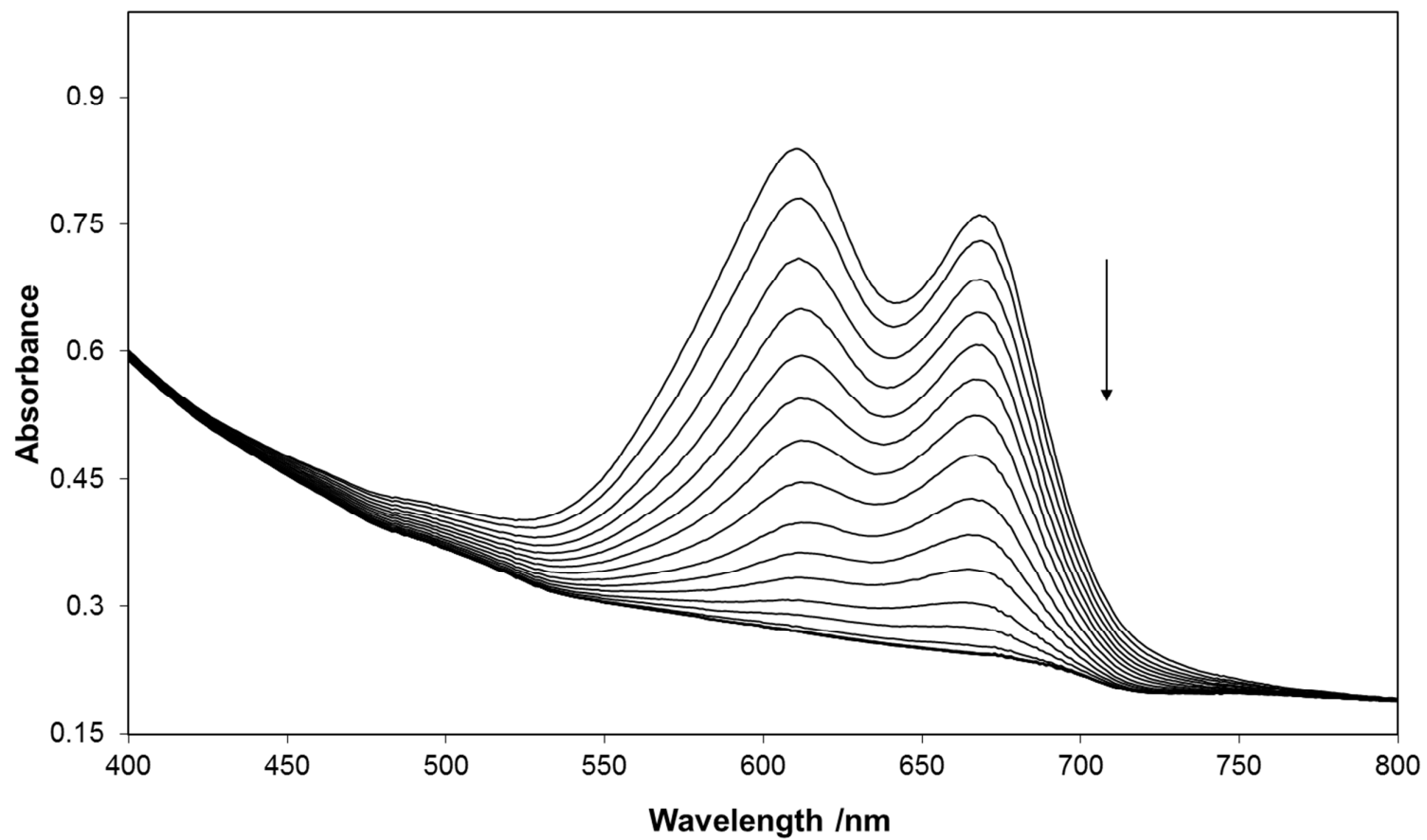
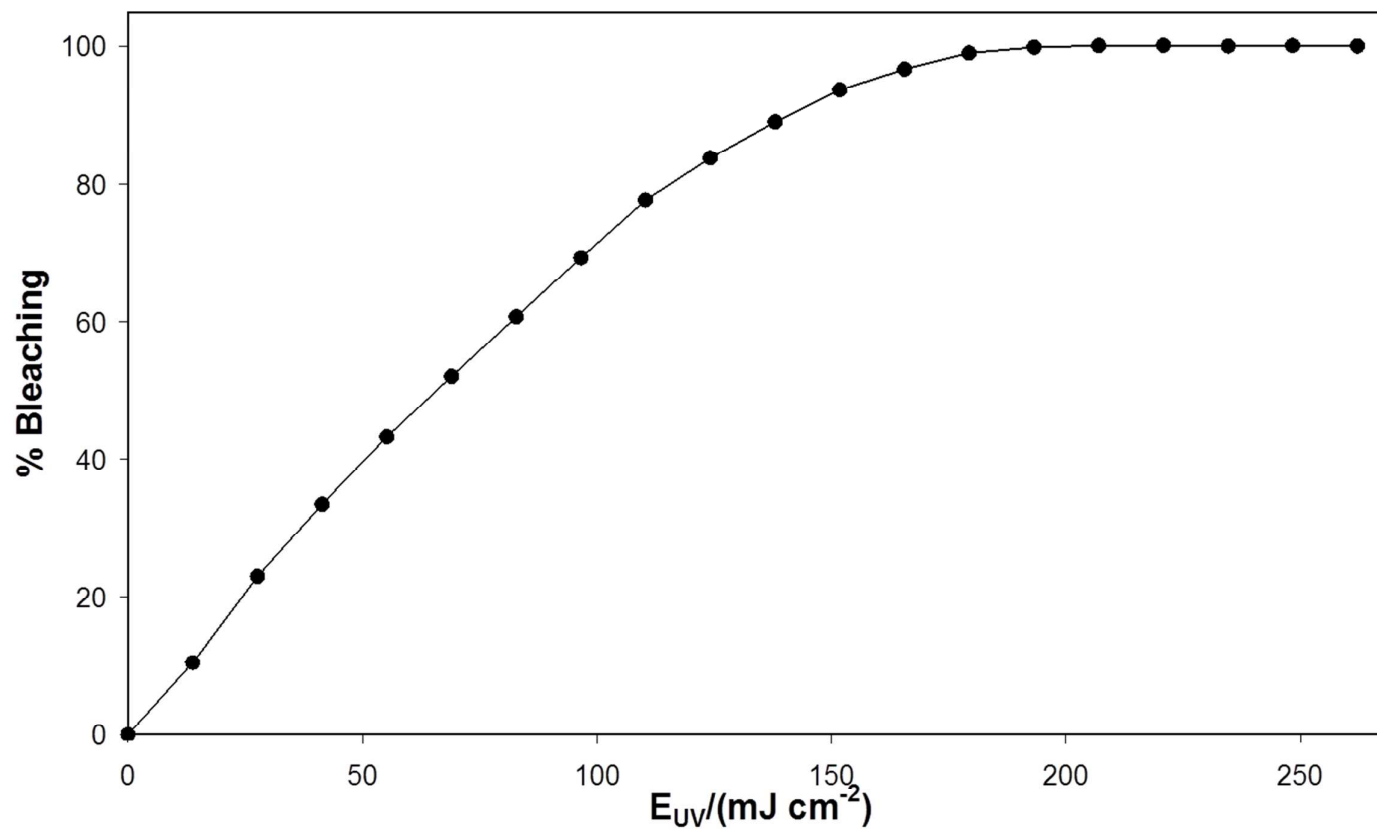


Fig. 10



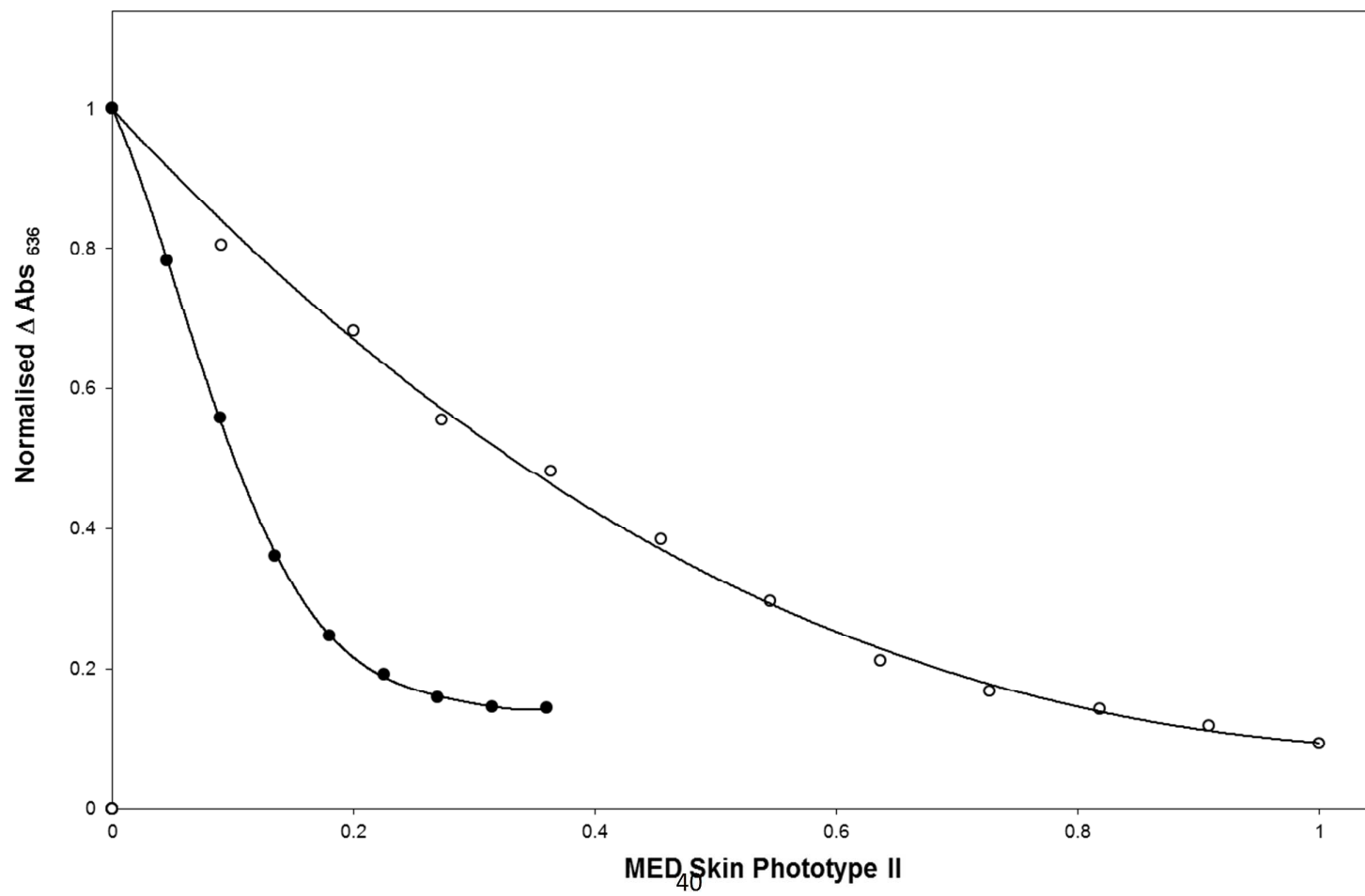
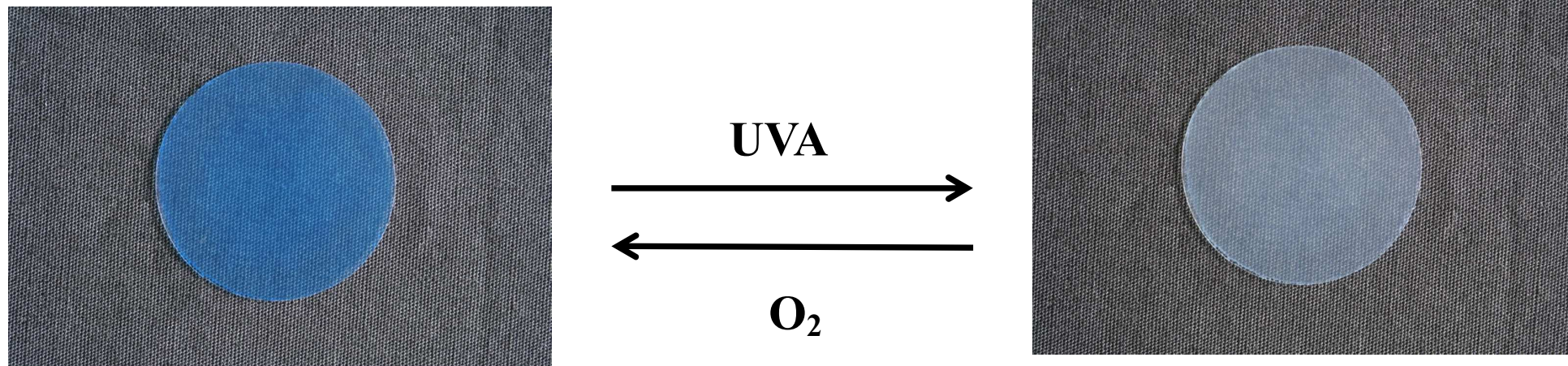


Fig. 12



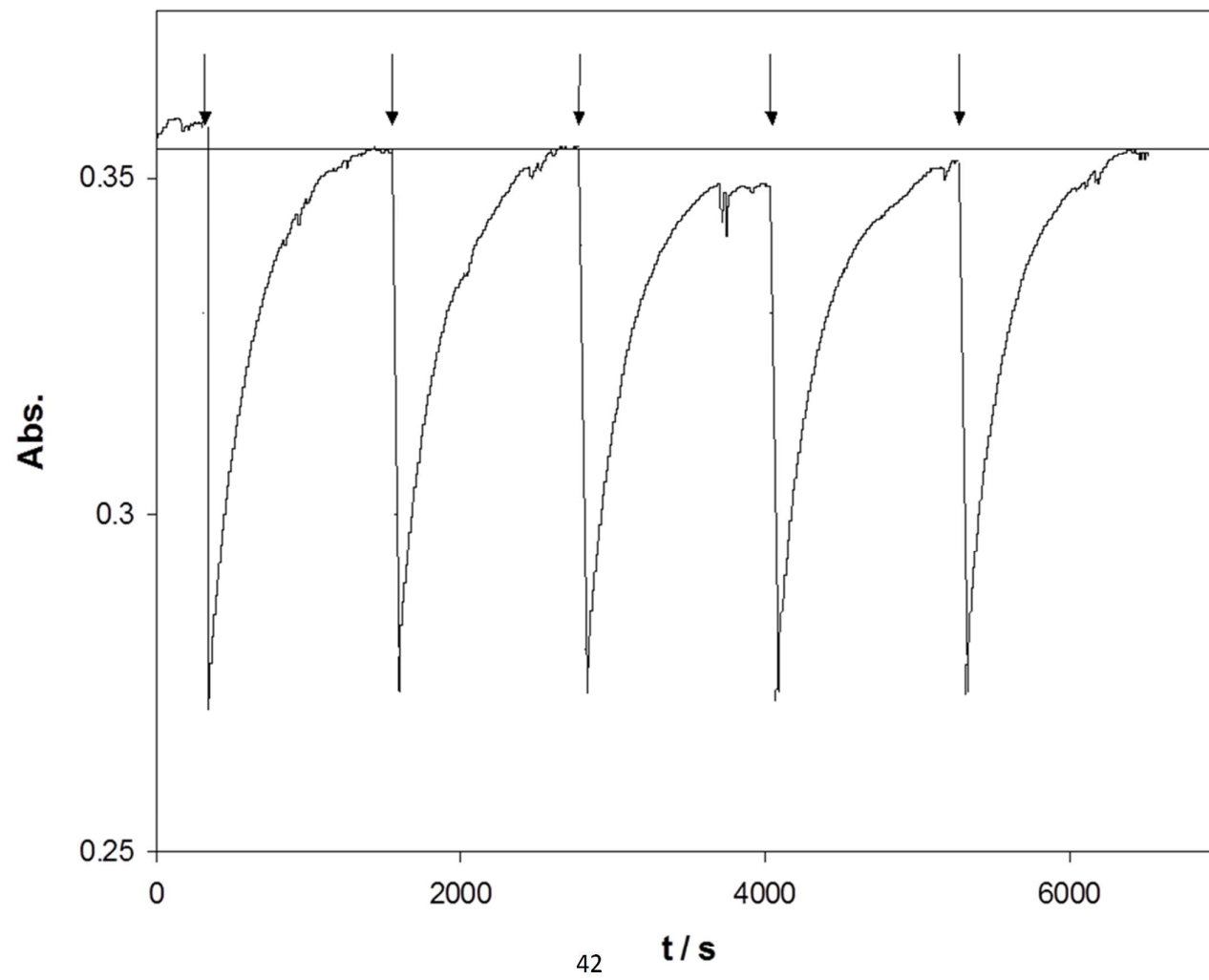


Fig. 14

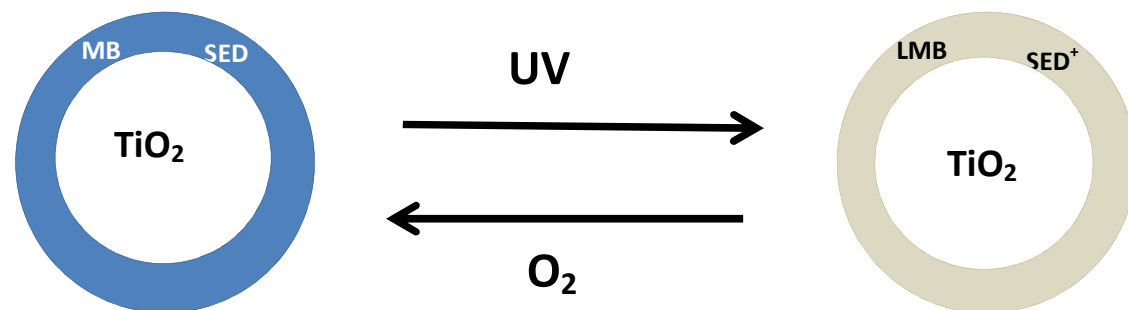


Fig. 15a

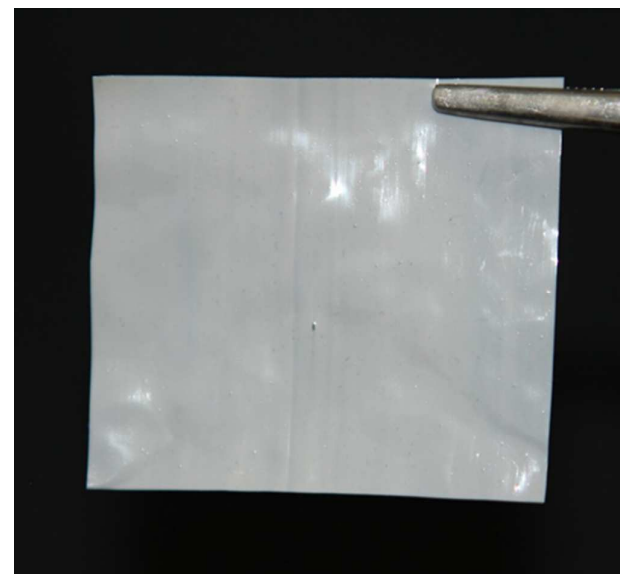
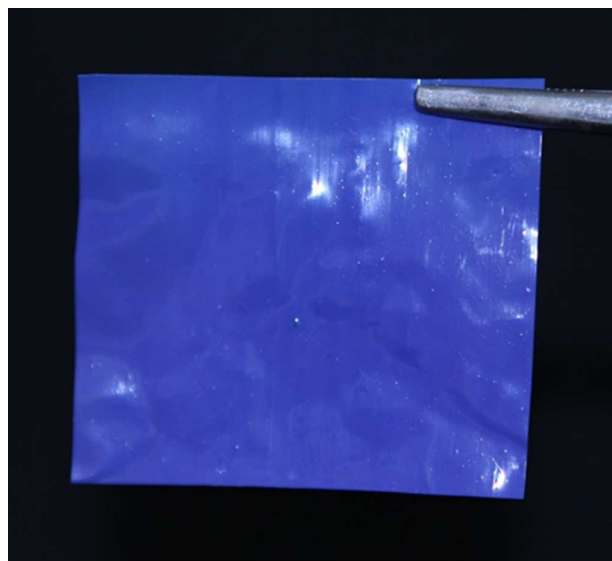
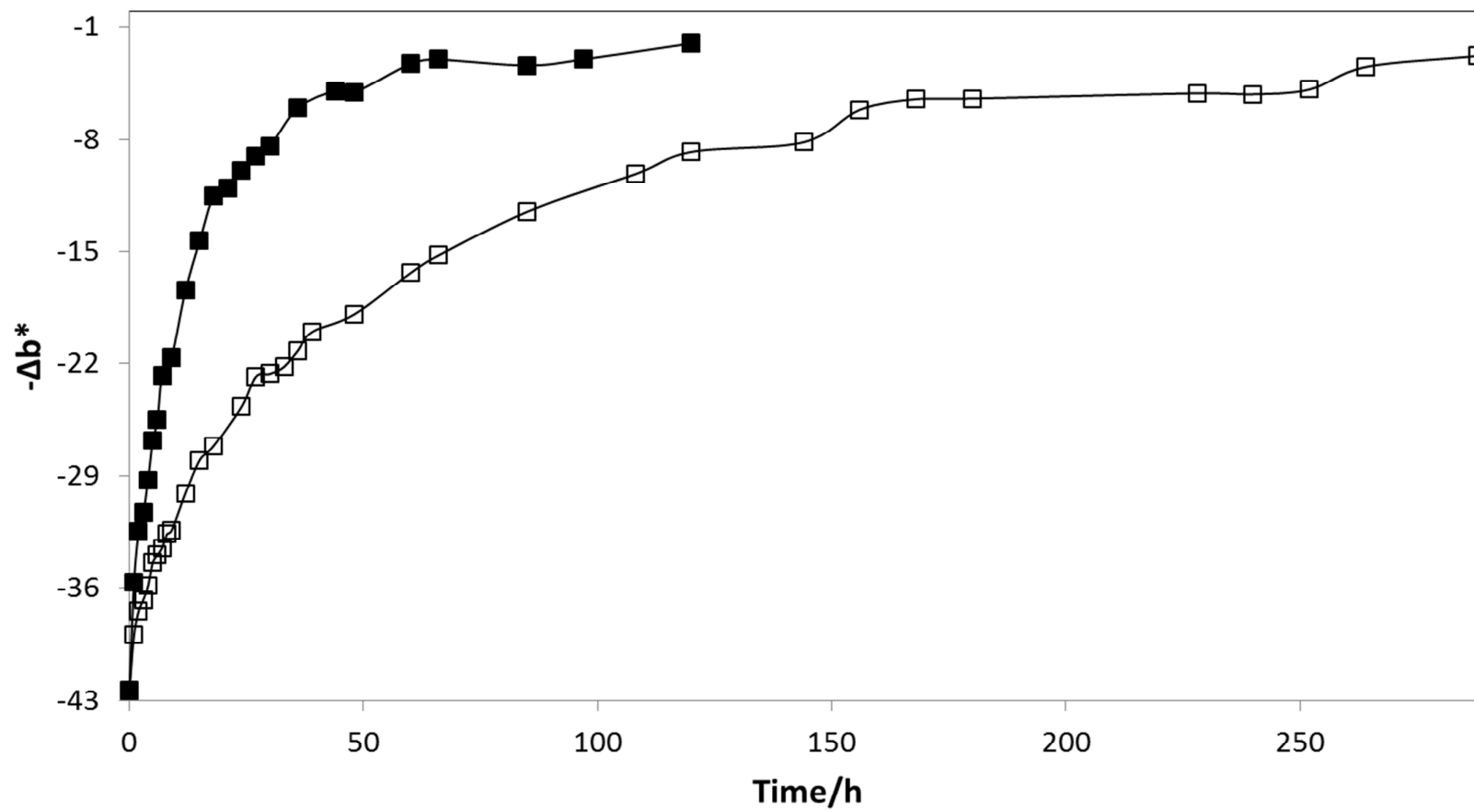


Fig. 15b



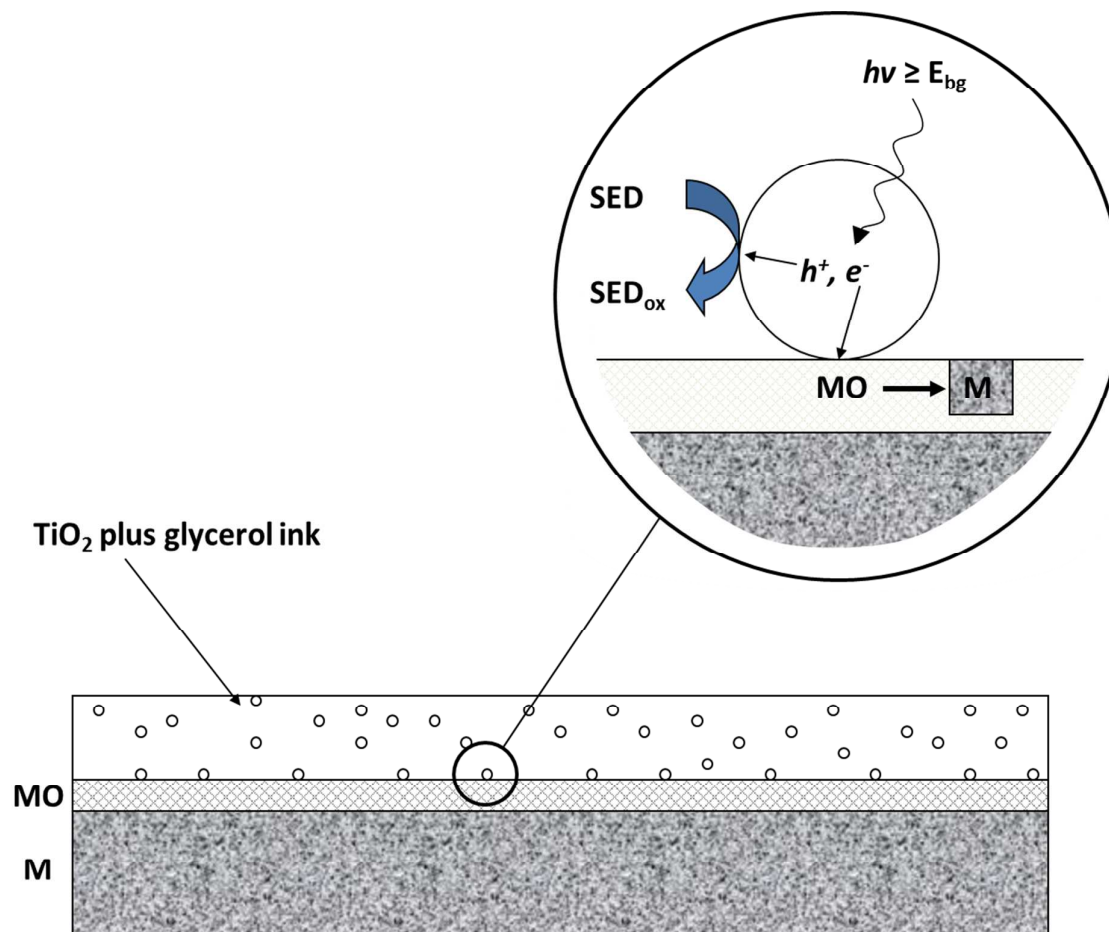


Fig. 17

